https://doi.org/10.5194/egusphere-2024-2576
Preprint. Discussion started: 19 September 2024

Revisiting the high tropospheric ozone over Southern Africa: overestimated biomass burning and underestimated anthropogenic emissions

Yufen Wang[1], Ke Li[1*], Xi Chen[1], Zhenjiang Yang[1], Minglong Tang[1], Pascoal M.D. Campos[2], Yang Yang[1], Xu Yue[1], and Hong Liao[1]

[1]Jiangsu Key Laboratory of Atmospheric Environment Monitoring and Pollution Control, Jiangsu Collaborative Innovation Centre of Atmospheric Environment and Equipment Technology, Joint International Research Laboratory of Climate and Environment Change, School of Environmental Science and Engineering, Nanjing University of Information Science and Technology, Nanjing, China
[2]CNIC-Centro Nacional de Investigação Científica, Ministério Do Ensino Superior Ciência, Tecnologia e Inovação, Avenida Ho Chi Minh N° 201, Luanda, Angola

Correspondence to: keli@nuist.edu.cn

Abstract. Tropospheric ozone over Southern Africa is particularly high and causes tremendous health risks and crop yield losses. It has been previously attributed to the influence by biomass burning (BB), with a minor contribution from anthropogenic emissions. However, due to the lack of measurements for ozone and its precursors, the modeled impacts of BB and anthropogenic emissions on tropospheric ozone were not well evaluated in Southern Africa. In this study, we combined the nested GEOS-Chem simulation with a horizontal resolution of 0.5° × 0.625° with rare multiple observations at the surface and from space to quantify tropospheric ozone and its main drivers in Southern Africa. Firstly, BB emissions from current different inventories exhibit similar peaks in summer season but also have large uncertainties in Southern Africa (e.g., uncertainty of a factor of 2-3 in emitted NO_x). The model-satellite comparison in fire season (July-August) in 2019 shows that using the widely used GFED4.1 inventory, the model tends to overestimate by 87% compared to OMI NO_2, while the QFED2 inventory can greatly reduce this model bias to only 34%. Consequently, the modeled tropospheric column ozone (TCO) bias was reduced from 14% by GFED4.1 to 2.3% by QFED2; the simulated surface MDA8 ozone was decreased from 74 ppb by GFED4.1 to only 56 ppb by QFED2. This suggests a highly overestimated role of BB emissions in surface ozone if GFED4.1 inventory is adopted. The model-observation comparison at the surface shows that the global CEDSv2 anthropogenic inventory tends to underestimate anthropogenic NO_x emissions in typical Southern African cities by a factor of 2-10 and even misrepresented anthropogenic sources in some areas. That means that urban ozone and $PM_{2.5}$ concentrations in Southern Africa may be strongly underestimated. For example, a ten-fold increase in anthropogenic NO_x emissions can change ozone chemistry regime and increase $PM_{2.5}$ by up to 50 μg m^{-3} at the Luanda city. Furthermore, we also find that the newly TROPOMI can already capture the urban NO_2 column hotspots over low-emission regions like Southern Africa while this is unavailable from the OMI instrument, highlighting the critical role of

https://doi.org/10.5194/egusphere-2024-2576
Preprint. Discussion started: 19 September 2024

high-quality measurements in understanding atmospheric chemistry issues over Southern Africa. Our study presents a quantitative understanding of the key emission sources and their impacts over Southern Africa that will be helpful not only to formulate targeted pollution controls, but also to enhance the capability in predicting future air quality and climate change, which would be beneficial for achieving a healthy, climate-friendly, and resilient development in Africa.

Keywords: biomass burning, tropospheric ozone, Southern Africa, urban emissions

1 Introduction

Tropospheric ozone (O_3) is an important trace gas in the atmosphere, posing multifaceted threatens to public health, crop yield, and global environment (Xu et al., 2018; Bourgeois et al., 2021). Complex photochemical oxidation of nitrogen oxides (NO_x = NO + NO_2) and volatile organic compounds (VOCs) in the presence of sunlight is the main source of tropospheric ozone (Wang et al., 2022). These two ozone precursors are emitted from both anthropogenic and natural sources. Great efforts have been made to reduce anthropogenic emissions, but ozone pollution is still challenging in many urban regions across the globe (Gaudel et al., 2020; Lyu et al., 2023). Globally, it was estimated that ~365,000 premature deaths could be attributed to ozone pollution in 2019 (Murray et al., 2020). The urban population exposed to ozone was increased at a trend of 0.8% per year from 2000 to 2019, and the largest increases of daily maximum 8-hour mean (MDA8) ozone occurred in Africa and India (Sicard et al., 2023). However, due to the lack of comprehensive studies on tropospheric ozone pollution in Southern Africa, it is urgent to explore the major source contributions driving ozone pollution over these less-studied regions. A better understanding of the major emission sources is not only helpful to formulate actionable targeted pollution controls and to reduce air pollution risks, but also important to predict future air quality in developing regions under the rapid changing of emissions and climate change.

Biomass burning (BB) emissions emit large amounts of air pollutants that are important ozone precursors (Qin et al., 2024). Africa is frequently exposed to intense BB (Vernooij et al., 2021), contributing to 70% of the global BB area and nearly 75% of global infant deaths attributed to BB pollutants (Jiang et al., 2020; Hickman et al., 2021). Exposure to air pollution from BB has strong differences in socioeconomic levels (Yue et al., 2024), with the most heavily exposed populations being in Southern Africa (Xu et al., 2023). Due to the complex climate types and unique lifestyles, BB in Africa during June-August months is concentrated over Southern Africa (Meyer-Arnek et al., 2005; Williams et al., 2010), and this "slash-and-burn" agricultural activity could lead to the very high ozone concentrations over Southern Africa. As shown in **Figure S1**, surface ozone concentrations in Southern Africa were simulated exceeding 100 ppb in July, making it to be the highest ozone level worldwide. This is consistent with the previous modeling findings that BB activities are the dominant driver of tropospheric ozone in this region (V. Clarmann et al., 2007). At the city level, Rwanda with observed daily ozone

https://doi.org/10.5194/egusphere-2024-2576
Preprint. Discussion started: 19 September 2024

maximum of 70 ppb during the dry season (Dewitt et al., 2019) can be affected by the transport of BB from Northern and Southern Africa. The high ozone is mainly driven by BB NO_x emissions; for example, the Southern African BB can increase NO_x concentrations by a factor of 2-5 in July-August months (Hoelzemann, 2006). Although BB has a great impact on ozone and its precursors in Southern Africa, there are few quantitative studies on this issue.

The popular way of quantifying the role of BB is to conduct chemical transport modeling, e.g., using the ECHAM5-MOZ (Aghedo et al., 2007), GEOS-Chem (Wang et al., 2022; Marvin et al., 2021), and WRF-Chem (Yang et al., 2022). The ECHAM5-MOZ model simulations show that BB can increase surface ozone by more than 50 ppb in Central Africa in June-August during 1997-2001 (Aghedo et al., 2007). Williams et al. (2010) used the Tracer Model version 4 to simulate June-August air pollution in 2006, and they showed that BB in Southern Africa is the largest source of carbon monoxide and ozone precursor emissions in Africa. However, model assessment is highly dependent on BB emission inventories and there is a lack of comparative studies of different BB inventories over the Southern Africa. This is because existing BB emission inventories have large uncertainties in Africa (Petrenko et al., 2012; Shi et al., 2015). The most widely-used inventory for global model simulations is the Global Fire Emissions Database (GFED) (Shi et al., 2020), and other BB inventories include the Quick Fire Emissions Database (QFED), the Global Fire Assimilation System (GFAS), and the Fire Inventory from NCAR (FINN). The uncertainties of a factor of 2-10 among these inventories source from estimated burned area, emission factors, and vegetation type (Fu et al., 2022). Depending on how fire emissions are calculated, these inventories can be divided into two categories: the fuel-based bottom-up estimation (e.g., GFED and FINN) (Pechony et al., 2013; Nikonovas et al., 2017) and the satellite-derived top-down estimation (e.g., QFED and GFAS) (Nikonovas et al., 2017). In addition, the injected height of BB emissions is also a key factor in determining the residence time of pollutants in the atmosphere that would impact the spatiotemporal distribution of tropospheric ozone (Rémy et al., 2017). Therefore, it is urgent to take advantage of observational constraints to evaluate the current BB inventories and quantify their impacts on tropospheric ozone in Africa.

In addition to the effects of BB, tropospheric ozone can be also affected by anthropogenic emissions in Africa. Although the intensity of anthropogenic emissions is relatively low in Africa, its impact at the urban scale cannot be ignored. With the rapid urbanization (Liousse et al., 2014), mean concentrations of surface SO_2, $PM_{2.5}$, and PM_{10} in Luanda have exceeded European Union human health protection limits (Campos et al., 2021). More importantly, anthropogenic emissions (e.g., black carbon) are projected to be comparable with BB emissions by 2030 in Africa (Liousse et al., 2014). Projection studies also pointed out that 50% of the population will be expected to live in cities by 2050 (Aucoin and Bello-Schünemann, 2016), resulting in a significant increase in the population exposure to ozone in Africa. With air pollution becoming a major cause of premature deaths in Africa (Julien et al., 2018), urban air pollution will likely pose more challenges in the context

https://doi.org/10.5194/egusphere-2024-2576
Preprint. Discussion started: 19 September 2024

of increasing anthropogenic emissions (Roy, 2016; Marais and Wiedinmyer, 2016; Zhang et al., 2021). However, whether the current anthropogenic emission inventories are reasonable in urban Southern Africa remains unclear.

Lack of surface observations is a major challenge for assessment of emission inventories in Africa. About 66% of African countries do not have regular air quality monitoring (Fajersztajn et al., 2014), particularly few in Southern Africa (Julien et al., 2018). Recently, there are continuous surface measurements available at several major cities over Southern Africa (**Figure 1**), together with the high-resolution satellite observations (e.g., TROPOMI), which could be very helpful to detect urban air pollution in this region. With the worsening air pollution in Africa (Sicard et al., 2023), it is particularly timely to take advantage of these valuable measurements to assess the key drivers of high tropospheric ozone in Southern Africa.

As abovementioned, there are notable uncertainties in the estimation of major emission sources over Southern Africa. The assessing and predicting the impacts of emissions on air quality and health risks rely heavily on model simulations, and these uncertainties in emission inventories can affect the development of effective control strategies. We therefore need to utilize surface and satellite observations to gain a comprehensive understanding of the emission source contributions in Southern Africa. This will help to develop effective mitigation measures to realize the Sustainable Development Goals for having a healthy, climate-friendly, and resilient development in Africa.

Here we integrated the high-resolution GEOS-Chem model and newly-available measurements to estimate the impact of biomass burning and anthropogenic emissions on tropospheric ozone over Southern Africa. The aim of this study is: 1) to identify the best estimate of BB emissions and quantify their impacts on regional tropospheric ozone over Southern Africa, and 2) to assess the representativeness of anthropogenic emission inventories in urban Southern Africa and their impacts on urban ozone pollution. Observational data, model description and experimental setup are presented in Section 2. Section 3.1 shows the major emission sources and the high tropospheric ozone issue over Southern Africa. The estimated impacts of biomass burning and anthropogenic emissions on tropospheric ozone are analysed in Sections 3.2 and 3.3, respectively. Conclusions and discussion are given in Section 4.

https://doi.org/10.5194/egusphere-2024-2576
Preprint. Discussion started: 19 September 2024

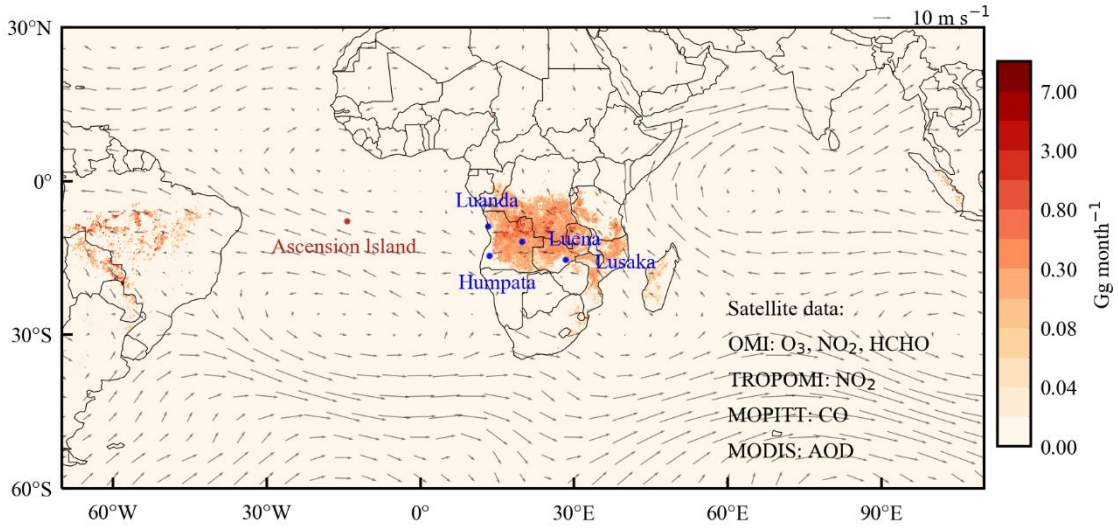

Figure 1. The biomass burning NO_x emissions (shaded) and 850hpa wind fields. The BB NO_x emissions are for July-August 2019 from the GFED4.1 inventory (unit: Gg month^{-1}). Blue dots represent the locations of surface observations and red dot denotes the ozonesonde measurement; and satellite data used in this study are listed in the lower right corner.

2 Measurement data and model description

2.1 Surface measurements

Figure 1 shows the locations of the four surface observation sites over Southern Africa. Hourly and daily real-time air quality indexes (AQI) for NO_2 and $PM_{2.5}$ were obtained from the Worldwide Air Quality Index (https://aqicn.org/station). The AQI can be converted to pollutant concentrations based on the website's AQI Calculator. There four sites record continuous measurement data in the study area, namely: Humpata in Angola (14°95'S, 13°44'E), Luanda in Angola (8°80'S, 13°23'E), Luena in Angola (11°76'S, 19°91'E), and Lusaka in Zambia (15°41'S, 28°29'E). The stations in Angola and Zambia have been operating since mid-May 2023 and February 2022, respectively, and data for June-August 2023 were selected for this study. To evaluate modeled ozone profiles, we adopted the Ascension Island's ozonesonde data from the Southern Hemisphere Additional Ozone Sounding (SHADOWZ) network (https://tropo.gsfc.nasa.gov/shadoz/), which measured ozone profile from 1998 (Thompson et al., 2000).

2.2 Satellite data

In order to investigate the model results driven by different BB emission inventories and the anthropogenic emission inventories, multiple observations from the OMI (https://disc.gsfc.nasa.gov/datasets/), TROPOMI

https://doi.org/10.5194/egusphere-2024-2576
Preprint. Discussion started: 19 September 2024

(https://www.earthdata.nasa.gov/sensors/tropomi), MODIS (https://ladsweb.modaps.eosdis.nasa.gov/search/), and MOPITT (https://giovanni.gsfc.nasa.gov/giovanni/) satellite instruments were used. Here, as listed in **Table S1**, we used tropospheric ozone, NO_2, and HCHO observations from OMI with resolutions of 1° × 1.25°, 0.25° × 0.25°, and 0.05° × 0.05°, respectively, as well as NO_2 observations from TROPOMI with a resolution of 0.125° × 0.125°. AOD and CO observations with a resolution of 1° × 1° are from MODIS and MOPITT, respectively.

2.3 Biomass burning emission inventories

In this study, six BB emission inventories were compared: GFED4.1, GFED5, GFAS, QFED2, FINNv1.5, and FINNv2.5. The GFED4.1 inventory provides dry matter emissions based on the area of BB and vegetation types from MODIS observations (Marvin et al., 2021; Zhang et al., 2018). The GFED5 is an updated version of GFED4.1 and the GFED5 global burned area is 61 % higher than GFED4.1 (Chen et al., 2023). The GFAS inventory estimates the amount of dry matter burning based on fire radiative power (FRP) (Vongruang et al., 2017). The QFED2 inventory is based on the FRP method and draws on the cloud correction method developed in GFAS with the high spatiotemporal resolution. FINNv1.5 calculates dry matter combustion using fire hot spots (FHS) data to calculate the burned area, and FINNv2.5 builds on this with extensive updates to the burned area, vegetation types, and chemicals emitted. In particular, FINNv2.5 adopted the active fire detections from the Visible Infrared Imaging Radiation Suite (VIIRS) to better capture small fires, and used multiple satellite products for daily fire emissions estimates (i.e., MODIS + VIIRS fire detections). The estimated BB NO_x emissions from these inventories will be further discussed in Section 3.2.1.

2.4 GEOS-Chem Model

The atmospheric composition in Africa was simulated by using the nested version of the three-dimensional global chemical transport model (GEOS-Chem, version 13.3.3; http://acmg.seas.harvard.edu/geos/), which was driven by the Modern-Era Retrospective analysis for Research and Applications version 2 (MERRA-2) meteorological reanalysis dataset. The model domain was for Africa (35°S - 30°N, 17°W - 50°E) with a horizontal resolution of 0.5° × 0.625° and a vertical configuration of 47 layers. The chemical boundary conditions for the nested simulation are provided by the global GEOS-Chem simulation with a horizontal resolution of 2° × 2.5°, which was updated every three hours. GEOS-Chem model includes fully coupled ozone-NO_x-hydrocarbon-aerosols chemistry mechanisms. $PM_{2.5}$ components include sulfate, nitrate, ammonium, dust, sea salt, organic carbon (OC), and black carbon (BC) (Park et al., 2004).

In Africa, anthropogenic emissions are from the Community Emissions Data System (CEDS) (Hoesly et al., 2018) and biogenic emissions are from the Model of Emissions of Gases and Aerosols from Nature (MEGAN) version 2.1 (Guenther et al., 2012). We simulated hourly concentrations of ozone, NO_2, and other pollutants in Africa for 2019-2023 using the

https://doi.org/10.5194/egusphere-2024-2576
Preprint. Discussion started: 19 September 2024

nested GEOS-Chem model with a set of sensitivity simulations (**Table 1**). In order to investigate the effect of BB on tropospheric ozone, we conducted three model experiments. Firstly, we used GFED4.1 and QFED2 to simulate the hourly concentrations of ozone, NO_2, HCHO, and CO for July-August, 2017-2019 (Run_GFED and Run_QFED), respectively, and validated the model results with satellite observations. Then, we conducted a sensitivity experiment by scaling down the QFED NO_x emissions to be consistent with satellite NO_2 observation (Run_QFED_34%). We used two different BB inventories and turned off aerosol chemistry to explore the effect of aerosols on ozone (Run_GFED_no-aerosol and Run_QFED_no-aerosol). We also explored the effect of emission height on simulated tropospheric ozone by emitting BB pollutants only within the PBL (Run_QFED_PBL).

After evaluating the BB emission inventories at the regional scale, we set up a series of experiments to explore the impact of anthropogenic emissions on tropospheric ozone in Southern Africa. Firstly, we used the up-to-date QFED inventory to simulate concentrations of NO_2 and $PM_{2.5}$ in June-August 2023 (Run_QFED_2023) and compared them with five surface air quality observations, and we also conducted model simulations for January-February 2020 (Run_QFED_2020) to explore the effect of anthropogenic emissions on tropospheric ozone during the non-fire season. It is noted that we fixed the anthropogenic emissions from CEDS at 2019 in all these simulations due to the lack of up-to-date anthropogenic emission data. Based on the underestimation of surface NO_2 observations in the model, we explored the sensitivity of ozone and $PM_{2.5}$ concentrations to anthropogenic NO_x changes by a factor of 10 or 20 over the Southern Africa (Run_QFED_Anth10NO_x and Run_QFED_Anth20NO_x); at the city scale, we explored the effects of perturbing anthropogenic NO_x emissions in Luanda by a factor of ten for difference sectors (i.e., power plant, industrial, and transportation) (Run_QFED_Anth_10NO_x _Sector).

Finally, we conducted two set of sensitivity simulations to attribute ozone to different emission sources, by turning off BB emissions, natural emissions (i.e., biogenic VOC and soil NO_x), and anthropogenic emissions, respectively (**Table 1**). In particular, we compared the ozone source attribution between the simulations by using the CEDS inventory and 10-fold CEDS NO_x emission.

https://doi.org/10.5194/egusphere-2024-2576
Preprint. Discussion started: 19 September 2024

Table 1. GEOS-Chem model simulations

	Experiments	BB emissions	Anthropogenic emissions
Impacts of biomass burning (July-August 2017-2019）	Run_GFED	GFED4.1	CEDSv2
	Run_QFED	QFED2	CEDSv2
	Run_QFED_66%NO_x	34% reduction in QFED2 NO_x emissions	
	Run_GFED_no-aerosol	Aerosol chemistry was turned off	
	Run_QFED_no-aerosol		
	Run_QFED_PBL	100% emissions below the PBL*	
Impacts of anthropogenic emissions	Run_QFED_2023	QFED2 June-August 2023	CEDSv2
	Run_QFED_Anth10NO_x		10-fold NO_x emissions
	Run_QFED_Anth20NO_x		20-fold NO_x emissions
	Run_QFED_Anth_10NO_x _Sector		10-fold NO_x emissions of energy, industry, and transportation sectors, respectively
	Run_QFED_2020	QFED2 January-February 2020	CEDSv2
Ozone source attribution （July-August 2019）	Run_QFED_noBB	BB emissions were turned off	
	Run_QFED_noNatl	BVOC and soil NO_x emissions were turned off	
	Run_QFED_noAnth	Anthropogenic emissions were turned off	
	Run_QFED_Anth10NO_x_noBB	BB emissions were turned off	
	Run_QFED_Anth10NO_x_noNatl	BVOC and soil NO_x emissions were turned off	
	Run_QFED_Anth10NO_x_noAnth	Anthropogenic emissions were turned off	

*The baseline simulation follows the vertical distribution of QFED2 emission (i.e., 65% emissions below the PBL and 35% emissions into the free atmosphere).

https://doi.org/10.5194/egusphere-2024-2576
Preprint. Discussion started: 19 September 2024

3. Results and discussion

3.1 Emission sources and simulated high ozone over Southern Africa

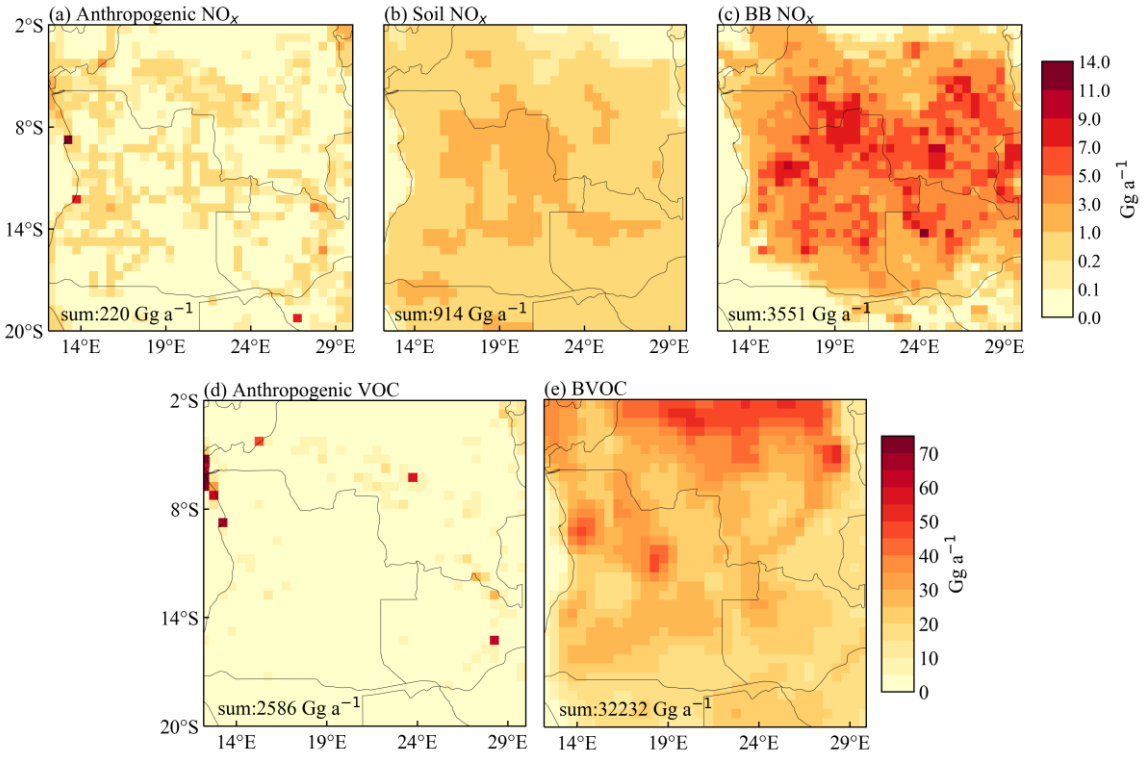

Figure 2. Spatial distributions of annual emissions of anthropogenic NO_x, soil NO_x, biomass burning NO_x, anthropogenic VOC, and BVOC in 2019 (unit: Gg a^{-1}). Anthropogenic NO_x, VOC from CEDSv2 inventory, soil NO_x and BVOC from Offline documents from GEOS-Chem official website, biomass burning NO_x from GFED4.1 inventory.

Figure 2 shows the annual emissions of anthropogenic NO_x, soil NO_x, BB NO_x, as well as anthropogenic VOCs (AVOC) and biogenic VOCs (BVOC) over Southern Africa in 2019, which were estimated at 220 Gg a^{-1}, 914 Gg a^{-1}, 3551 Gg a^{-1}, 2586 Gg a^{-1}, and 32,232 Gg a^{-1}, respectively. It should be noted that here BB NO_x emissions are from the GFED4.1 inventory. In terms of NO_x emissions, BB emission is the largest contributor and is about 16 times of NO_x emissions from anthropogenic sources. The regions with high anthropogenic emissions are mainly Luanda, Kinshasa, and Lusaka which are the capitals of Angola, the Democratic Republic of the Congo (DRC), and Zambia, respectively. High vegetation cover in Southern African region leads to high BVOC emissions which are about 12 times of AVOC emissions. Seasonally, **Figure 3** presents the monthly variations of ozone precursor emissions averaged over Southern Africa in 2019. The BVOC

https://doi.org/10.5194/egusphere-2024-2576
Preprint. Discussion started: 19 September 2024

emission exhibits a strong seasonal pattern ranging from 2000 Gg month^{-1} to 4000 Gg month^{-1}, and it peaks in March and then decreases to the minimum in July-August. This seasonality is consistent with the seasonal variation in isoprene emissions in Southern Africa in 2006 as reported by Williams et al. (2009). We can also see that NO_x from BB peaks during June-August, which is consistent with the results of Boschetti and Roy (2008). Emissions of BB NO_x in January-April and November-December were relatively small. The seasonal contrast in BB NO_x and BVOC emissions highlights the importance of BB in the production of high summer tropospheric ozone in this region (Vieira et al., 2023).

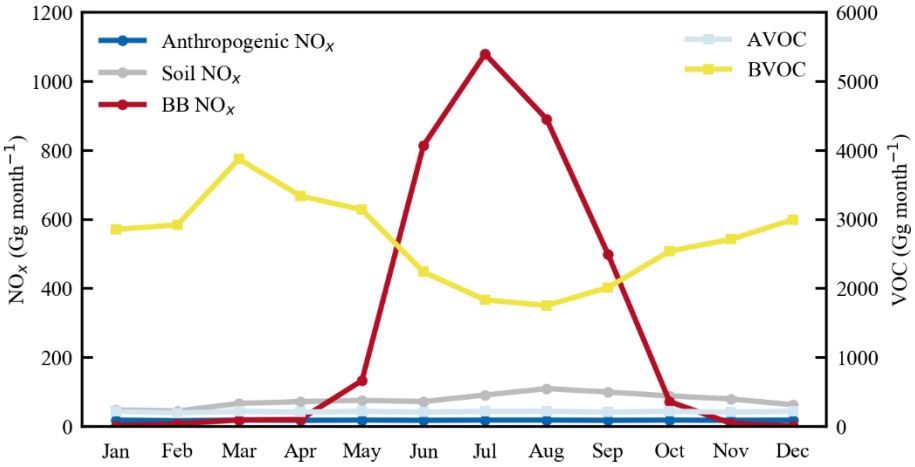

Figure 3. Seasonal variations in anthropogenic NO_x (deep blue), soil NO_x (grey), biomass burning NO_x (red), anthropogenic VOC (blue), and biogenic VOC (yellow) emissions in 2019 (unit: Gg month^{-1}). Anthropogenic NO_x, VOC from CEDSv2 inventory, soil NO_x and BVOC from Offline documents from GEOS-Chem official website, biomass burning NO_x from GFED4.1 inventory.

Figure 4a shows the simulated spatial distribution of MDA8 ozone in July-August of 2019 in Africa by using the GEOS-Chem model with the GFED4.1 inventory (Run_GFED). The regional average of MDA8 ozone in Southern Africa is about 74 ppb and the maximum can be up to 120 ppb in northern Angola and southwest Congo. Dewitt et al. (2019) observed a daily ozone maximum of 70 ppb during the dry season in Rwanda, which is adjacent to the DRC. Based on our simulation

https://doi.org/10.5194/egusphere-2024-2576
Preprint. Discussion started: 19 September 2024

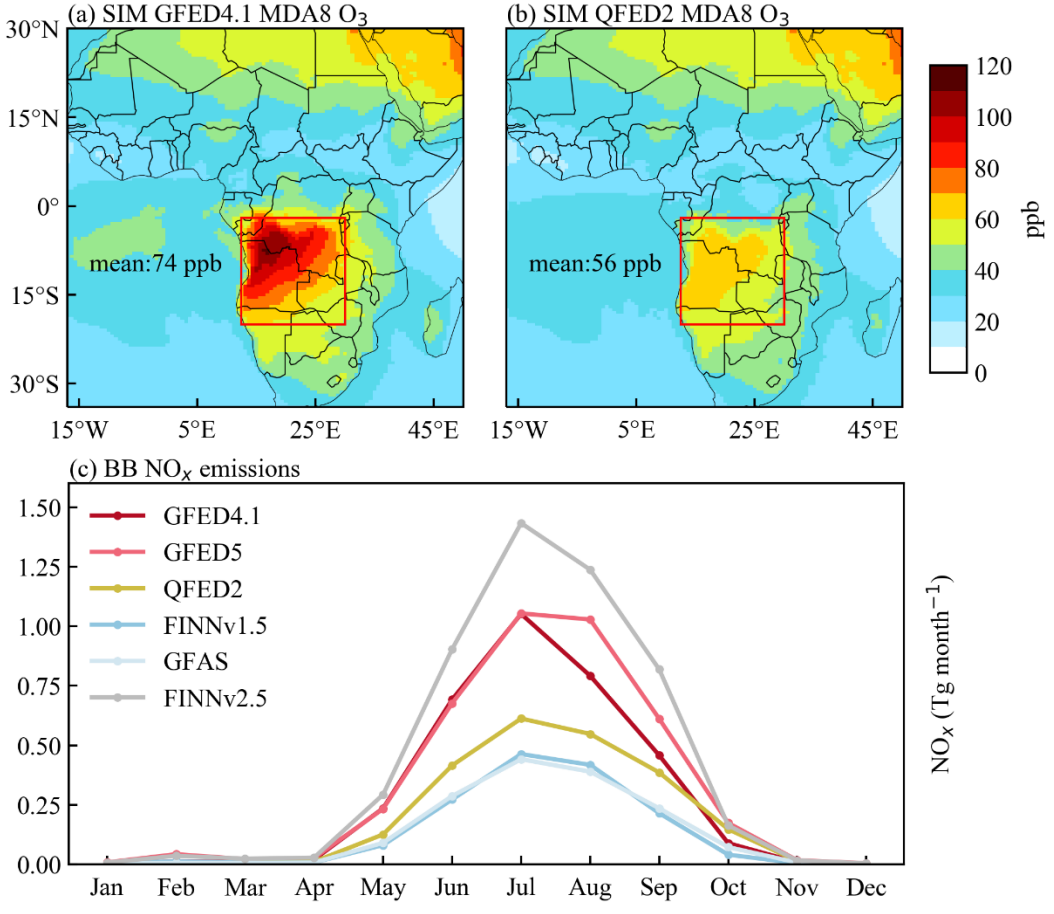

Figure 4. Differences in BB NO_x emissions and modeled surface ozone from different inventories. (a-b) Surface MDA8 ozone simulated by GEOS-Chem model for July-August 2019 by the GFED4.1 and QFED2 inventories, respectively. (c) Monthly BB NO_x emissions in 2014 averaged over the Southern African region.

results, it can be found that the daily maximum ozone during the BB season is 86 ppb for Rwanda. This comparison indicates an overestimation in the baseline simulation (Run_GFED). **Figure 5a** shows the spatial distribution of simulated tropospheric column ozone concentrations (TCO), with maximum values of up to 50 DU mainly in northern Angola and southwest Congo. Higher TCO levels are also seen over the Atlantic Ocean, which are mainly associated with long-range transport (Williams et al., 2010; Meyer-Arnek et al., 2005). The above results confirm that BB contributes greatly to high ozone concentrations during the fire season in Southern Africa. As such, a better understanding of the high ozone over Southern Africa would depend on the accurate estimate of BB emissions.

https://doi.org/10.5194/egusphere-2024-2576
Preprint. Discussion started: 19 September 2024

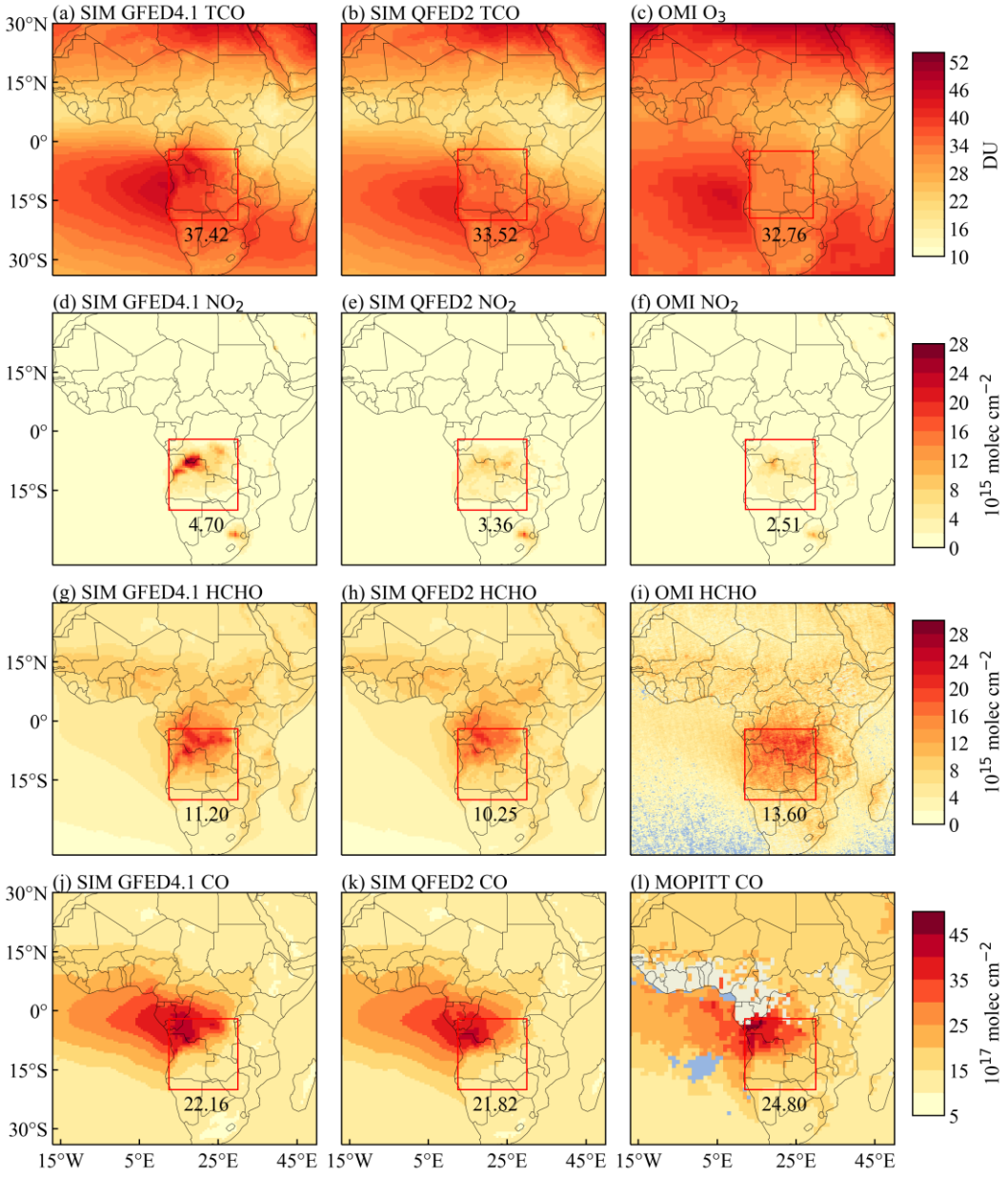

Figure 5. The comparison of GEOS-Chem simulated (left and middle panels) and satellite-based (right panels) tropospheric columns for ozone and its precursors. The simulated TCO, NO_2, HCHO, and CO columns in Africa for July-August 2019 were driven by the GFED4.1 and QFED2 inventories, respectively. For CO satellite data, only the July value was used due to the large amount of missing measurement in August. The numbers in the figure are the mean values in the red boxed area.

https://doi.org/10.5194/egusphere-2024-2576
Preprint. Discussion started: 19 September 2024

3.2 Impacts of biomass burning (BB) on tropospheric ozone

3.2.1 Uncertainties in BB emission inventories

Although the GEOS-Chem model has been widely employed for modeling tropospheric ozone globally (Balamurugan et al., 2021; Li et al., 2023), its evaluation against measurements over Southern Africa is very limited. In order to accurately evaluate the effects of BB emissions on tropospheric ozone, we need to take the uncertainties from different BB emissions into account (Wiedinmyer et al., 2023).

Figure 4c shows the monthly emissions of BB NO_x in 2014 for the Southern Africa from the six emission inventories (GFED4.1, GFED5, QFED2, GFAS, FINNv1.5, and FINNv2.5). All of the six BB inventories share the similar seasonality in NO_x emissions, but there are large differences with a factor of 2-3 in estimated emission intensities, particularly in the dry season. The inventory was divided into two groups based on the level of emissions, with the high emission groups being FINNv2.5, GFED5, and GFED4.1. FINNv2.5 shows the highest BB NO_x emissions, which are 45% higher than GFED4 emissions and 130% higher than QFED2 emissions, but Wiedinmyer et al. (2023) also suggests that FINNv2.5 probably tends to overestimate NO_x emissions in Africa. GFED5 is an updated version from GFED4.1, and their difference in NO_x emissions is minimum in January-July and enlarged in August. The low emission groups are: QFED2, GFAS, and FINNv1.5. GFAS and FINNv1.5 resemble in the estimated NO_x emissions but both of them are significantly lower than the other inventories. This may be attributed to the underestimated burned area and emissions in FINNv1.5 (Wiedinmyer et al., 2011). Therefore, in the following, we will use the GFED4.1 and QFED2 inventories to represent the high estimate and low estimate of BB NO_x emissions for Southern Africa, respectively.

3.2.2 Simulated tropospheric ozone with different BB emissions

Figures 4a-4b show the simulated spatial distribution of MDA8 ozone in Africa during the fire season (July-August) in 2019 by using the GEOS-Chem model with the GFED4.1 and the QFED2 inventories, respectively. The simulated surface MDA8 ozone by the GFED4.1 inventory is 74 ppb over Southern Africa, which is 32% higher than the value of 56 ppb by the QFED2 inventory. The maximum value of MDA8 ozone by the GFED4.1 inventory can reach up to 120 ppb, but the maximum value by he QFED2 inventory is only 70 ppb. This remakable discrpancy suggests that the uncertainties of surface ozone over Southern Afria are largely dependent on BB emissions. For the tropospheric ozone, **Figures 5a-5b** show the simulated spatial distribution of TCO by using the GFED4.1 and QFED2 inventories. In contract to surface ozone, the regional average of TCO simulated by the GFED4.1 inventory is only 4 DU (11%) higher than that simulated by the QFED2 inventory.

To evaluate whether the model performance in the vertical profile of tropospheric ozone in Africa, we compared the model

https://doi.org/10.5194/egusphere-2024-2576
Preprint. Discussion started: 19 September 2024

results with ozonesonde observations from Ascension Island, UK (7°96'S, 14°91'W) in **Figure 6**. As shown in **Figure 1**, Ascension Island is located downwind of the high BB area, and ozone and its precursors from BB can be transported from Southern Africa to the South Atlantic (Mari et al., 2008), leading to ozone enhancement in Ascension Island (Jenkins et al., 2021). The ozone concentrations modeled by GEOS-Chem respond well to the ozonesonde observations in terms of vertical distribution, and in particular the model captures the variation in observations with altitude well. The differences in ozone concentrations due to the two BB inventories are small in vertical distribution, and are mainly concentrated below 1.5 km with ozone concentrations differing by about 3 ppb. This is consistent with the results of small TCO differences in **Figures 5a-5b**. Compared to the ozonesonde observations, GEOS-Chem captures the ozone variations well regardless of which inventory is used.

3.2.3 Satellite constraints on BB emission estimates

In order to evaluate the tropospheric ozone simulation in Africa region, in **Figure 5** we compared the simulated columns with GFED4.1 and QFED2 inventories against satellite observations of TCO and ozone precursors (e.g., NO_2, CO, and HCHO). The simulated TCO with GFED4.1 inventory shows high values of up to 50 DU near the fire source regions in northern Angola and southern DRC, and in the downwind region over Atlantic Ocean. The OMI TCO has the regional average of 37.4 DU, suggesting an overestimation of 14% in the GFED4.1 simulation relative to OMI. In contrast, the simulated TCO with QFED2 inventory is strongly spatially consistent with the OMI satellite, with a slight overestimation of 2.3%.

Figures 5d-5e show the simulated and observed tropospheric NO_2 columns. The GFED4.1 inventory simulation exhibits high value of up to 28×10^{15} molecule cm^{-2} near the BB source region, but there is a large overestimation of 87% with respect to the OMI satellite data. Similar conclusions are also from Anderson et al. (2021) that the model using the GFED4.1 inventory can capture high NO_2 in Africa but the bias was as high as 100%. This is in agreement with previous studies that model simulations trend to produce a high bias towards BB activities in Africa (Souri et al., 2024). However, the QFED2 inventory simulation can greatly reduce this high bias, with an overestimation of only 34%. In **Figure S2**, we also compared model results with the TROPOMI satellite, and a similar high bias was also found in the modeled NO_2 columns. If we further have QFED2 NO_x emissions reduced by 34%, as shown in **Figure S3**, it can effectively reduce the bias for NO_2 columns from 34% to 0.4% and reduce the overestimation of the TCO columns to 1.1%. This sensitivity simulation demonstrates the importance role of BB NO_x emissions in tropospheric ozone production.

https://doi.org/10.5194/egusphere-2024-2576
Preprint. Discussion started: 19 September 2024

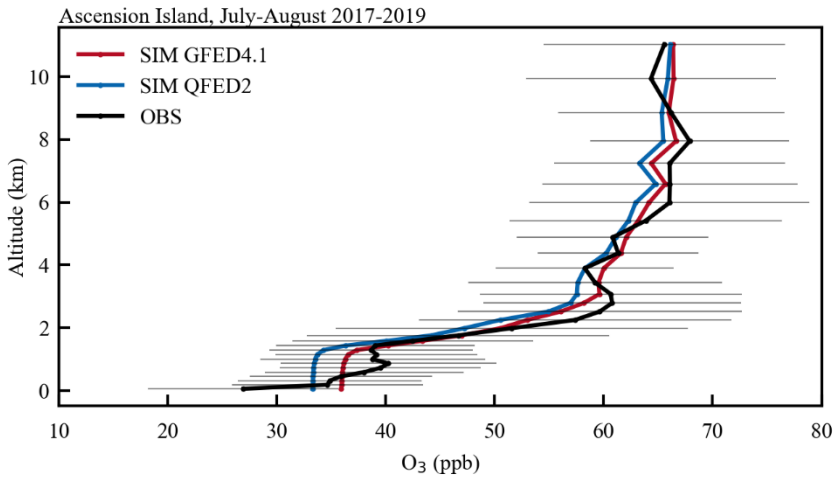

Figure 6. The comparison of GEOS-Chem simulated and measured vertical ozone distributions over the Ascension Island, UK, for July-August 2017-2019. The model results by the GFED4.1 (red) and QFED2 (blue) inventories are both given.

Figures 5g-5i show the simulated and satellite-derived tropospheric HCHO columns. The HCHO column concentrations simulated by GEOS-Chem are generally consistent with satellite observations, with high values of up to more than 20 × 10^{15} molecule cm^{-2} in northern Angola and southwest DRC. Simulated HCHO column concentrations between the GFED4.1 and QFED2 inventories were consistent spatially, with only a difference of 1 × 10^{15} molecule cm^{-2} on a regional basis. The levels and spatial distributions of HCHO are mainly influenced by BVOC and BB emissions. Firstly, the Congo Basin, as one of the largest tropical rainforests, emits a large amount of BVOCs that can be oxidized to generate high values of HCHO (Wells et al., 2020). It leads to the spatial distribution of HCHO similar to the distribution of BVOC sources. Secondly, BB is found to be one of the main sources of HCHO in the African continent (Liu et al., 2020). Differences in VOC and NO_x emissions between GFED4 and QFED inventories (Van Der Werf et al., 2017), e.g., BB VOC emissions in GFED4.1 being two times of the QFED2 inventory in 2019, may account for the slightly different HCHO columns.

The simulated CO columns in **Figures 5j-5l** are spatially similar to MOPPIT retrievals, with high values in the downwind regions of fire sources. The regional average of CO column concentrations simulated by GEOS-Chem is underestimated by approximately 10% compared to MOPITT. Hoelzemann (2006) used a variety of BB emission inventories to drive the MOZART model to simulate CO concentrations in Southern Africa in September-October 2000, and they showed that all simulations exhibited an underestimation against the MOPITT CO. In addition, we also found that the simulated spatial distribution of CO columns is similar with each other among different BB inventories, and their regional difference is only 1%. This suggests that neither HCHO nor CO is the main reason for the overestimation of ozone production.

https://doi.org/10.5194/egusphere-2024-2576
Preprint. Discussion started: 19 September 2024

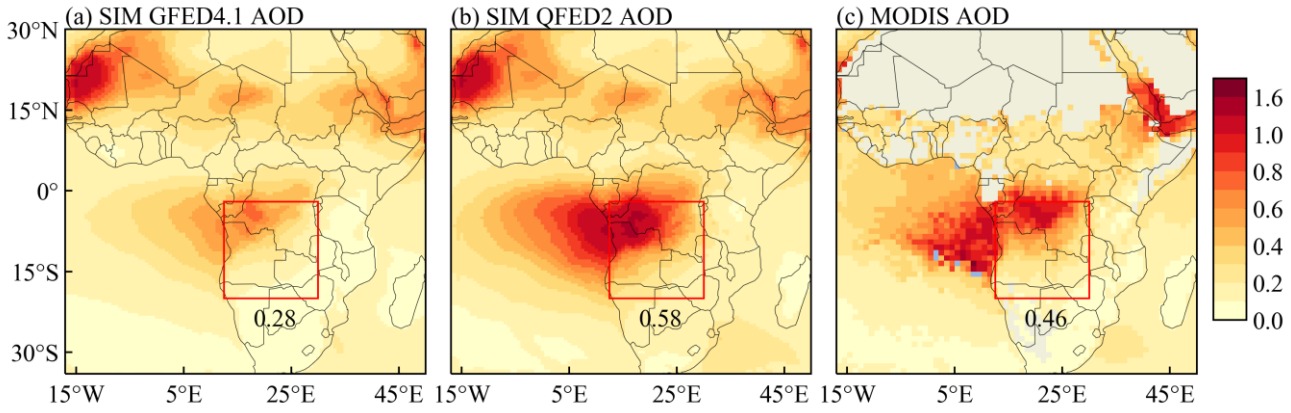

Figure 7. The comparison of GEOS-Chem simulated AOD in Africa in July-August 2019 with the MODIS AOD. The model results by the GFED4.1 (left) and QFED2 (middle) inventories are both given.

Figure 7 shows the spatial distribution of modeled and satellite-based AOD. The simulation results by both inventories can capture the spatial variability of MODSI AOD. But simulated regional mean AOD by the QFED2 inventory overestimated MODIS AOD by 26%, while the GFED4.1 inventory underestimated MODIS AOD by 37%. Tian et al. (2019) used GFED4 as an input to drive the GEOS-Chem model and also showed that the model tended to underestimate the intensity and spatial distribution of AOD in the African region. The inconsistency between these two inventories may be attributed to the discrepancy in carbonaceous aerosol emissions, since the OC and BC emissions from GFED4 are only half of the QFED emissions (Chang et al., 2023). In addition, the difference between OC and BC in the biomass burning emission inventories could affect ozone simulation through aerosol chemistry, and the results are shown in **Figure S4**. After turning off aerosol chemistry alone in the model, regional surface ozone was increased by 10 ppb and TCO by 2 DU using the GFED4.1, while using the QFED2 regional ozone was increased by 14 ppb and TCO by 4 DU. As such, the lower level of aerosols in GFED4.1 may be a reason for the overestimation of simulated ozone concentrations.

In conclusion, the widely-used GFED4.1 inventory has a large bias in simulating tropospheric ozone in Southern Africa, and the QFED2 inventory exhibit much more consistent with satellite observations. This bias is mainly due to the overestimation of NO_x emissions in Southern Africa in GFED4.1. Firstly, NO_x emissions in GFED4.1 are 38% higher than in QFED2 in Southern Africa. Secondly, the modeled NO_2 column in GFED4.1 shows a high bias compared to QFED2 and satellite observations, while the modeled HCHO and CO columns are generally consistent between GFED4.1 and QFED2 inventories. Thus, we conclude that the overestimation of ozone in Southern Africa simulated with GFED4.1 is due mainly to the overestimation of NO_x and the lower aerosol levels in GFED4.1 may be a minor reason for the overestimation of modeled ozone concentrations. We will use the QFED2 inventory for BB emissions in the following

https://doi.org/10.5194/egusphere-2024-2576
Preprint. Discussion started: 19 September 2024

analysis.

3.2.4 Role of BB emission heights in ozone simulation

The representativeness of BB emission injection heights is also an important factor that can impact ozone simulations (Rémy et al., 2017). We conducted a sensitivity experiment using the QFED2 inventory and allowed all BB emissions emitting below the PBL. As shown in **Figure 8**, the impact of this vertical partitioning on surface ozone varies regionally. At the surface, the changes of MDA8 ozone were within ± 2.4 ppb and the BB source areas showed a decreased ozone. For TCO, the simulated mean values with this vertical partitioning were 0.2 DU higher than those without vertical partitioning, but the magnitude of this effect is smaller than the TCO changes (~4 DU) caused by the difference in BB NO_x emissions between GFED4.1 and QFED2 inventories. Thus, our simulations demonstrate that the configuration of BB emission height has a limited effect on surface ozone level but a moderate influence on TCO columns in this region.

3.3 Impacts of anthropogenic emissions on tropospheric ozone

3.3.1 Uncertainties in anthropogenic emission inventories

Uncertainties may exist in anthropogenic emissions from regional scale to urban cities in Southern Africa. For example, in **Table 2** we compared the differences in NO_x emissions between two widely-used global inventories: CEDSv2 and HTAPv3. Whether in Southern Africa or Luanda, there is a missing seasonality in NO_x emissions in CEDSv2, whereas NO_x emissions in HTAPv3 are much higher in January-February than in other months. Over the Southern Africa, monthly NO_x emissions in the CEDSv2 are about 30% lower than the HTAPv3 in January-February. For Luanda, the CEDSv2 inventory is 87% lower than HTAPv3 in January-February 2018 and 20-50% lower in the other months. In addition, the validation of anthropogenic emission in global inventories was barely evaluated in this region and we will take advantage of recently available surface measurements and satellite retrievals to fill this gap.

3.3.2 Model evaluation against surface measurements of NO_2 and $PM_{2.5}$

Currently, there are very few surface observations in Southern Africa. However, in the study, there are three cities (Humpata, Luanda, and Luena) that have continuous surface measurements of NO_2 during the period of June-August 2023, and four cities (Humpata, Luanda, Luena, and Lusaka) with surface measurements of $PM_{2.5}$. These measurements are critical to understand the hotspots of urban anthropogenic emissions as indicated in **Figure 2a**. Luanda is the capital of Angola with dense population, and the median surface NO_2 concentrations observed at this station ranged from 10 ppb to 30 ppb. The

https://doi.org/10.5194/egusphere-2024-2576
Preprint. Discussion started: 19 September 2024

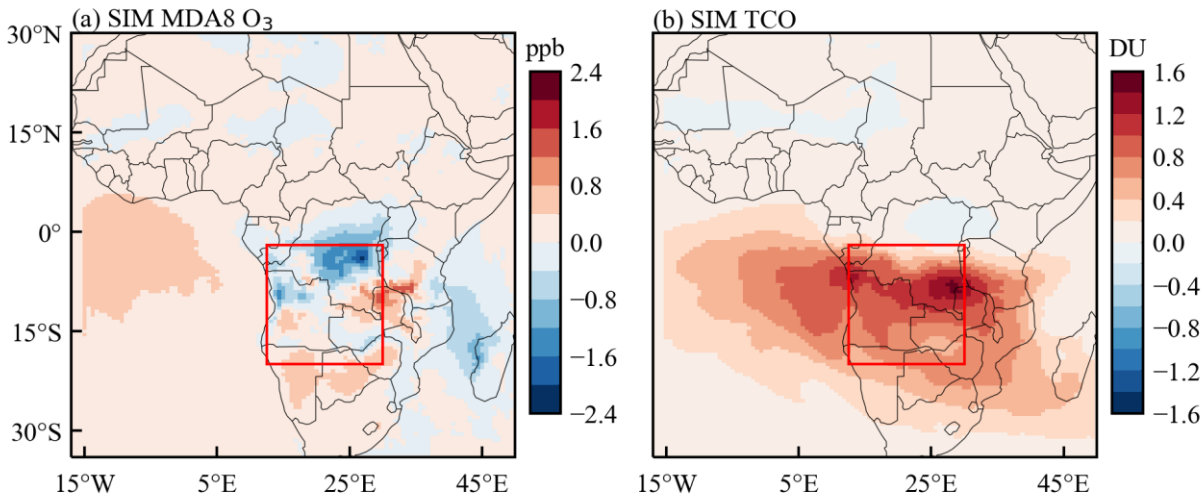

Figure 8. Effects of vertical partitioning of model BB emissions in surface MDA8 ozone and tropospheric ozone columns. The baseline simulation follows the vertical distribution of QFED2 emission (i.e., 65% emissions below the PBL and 35% emissions into the free atmosphere), and the sensitivity simulation allows 100% BB emissions emitted below the PBL. Here the plots are the differences between the baseline simulation (Run_QFED) and sensitivity simulation (Run_QFED_PBL).

Table 2. Monthly anthropogenic NO_x emissions in Southern Africa and Luanda (unit: Gg month^{-1}).

		Jan.	Feb.	Mar.	Apr.	May	Jun.	Jul.	Aug.	Sep.	Oct.	Nov.	Dec.
Southern Africa	CEDSv2	18.2	16.5	18.2	17.6	18.2	17.6	18.2	18.2	17.6	18.2	17.6	18.2
	HTAPv3	27.1	24.9	17.6	17.0	17.3	18.9	19.0	17.1	16.7	17.8	17.0	16.4
Luanda	CEDSv2	0.8	0.7	0.8	0.8	0.8	0.8	0.8	0.8	0.8	0.8	0.8	0.8
	HTAPv3	6.3	5.2	1.5	1.0	1.2	1.1	1.1	1.2	1.0	1.3	1.2	1.0

Humpata station is located at Universidade Privada de Angola, where the observed NO_2 concentrations ranged from 5 ppb to 25 ppb, with large day-to-day variations of up to 20 ppb. The Luena station is located in a residential area of Luena, where the observed NO_2 concentrations were much higher than those of the previous two stations, with a maximum of 50 ppb. **Figure 9** shows the comparison of the observed and simulated daily surface NO_2 concentrations in Luanda, Humpata, and Luena, respectively. Compared with the observed values, the modeled NO_2 concentrations for all three cities are much

https://doi.org/10.5194/egusphere-2024-2576
Preprint. Discussion started: 19 September 2024

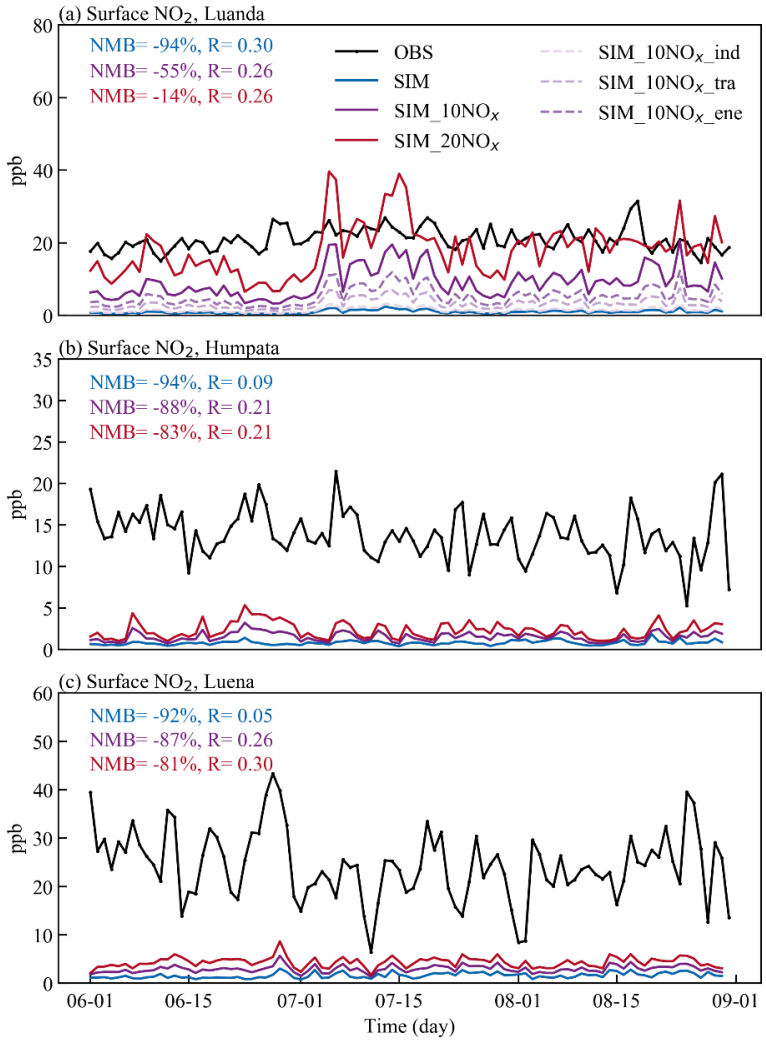

Figure 9. Time series of simulated and observed daily median surface NO_2 concentrations in Southern African cities (Luanda, Humpata, Luena) in June-August 2023. The model was driven by the QFED2 inventory and fixed CEDSv2 inventory in 2019. The "SIM" denotes the baseline simulation (Run_QFED_2023), and "SIM_10NO_x", and "SIM_20NO_x" denote the 10-fold and 20-fold increase in NO_x emissions from CEDSv2. The dashed lines indicate a 10-fold increase in NO_x emissions from the energy (ene), industry (ind) and transportation (tra) sectors, respectively, in the CEDSv2 inventory.

lower than the observed values, underestimated by 90%. There is also a large underestimation of surface NO_2 in Luanda compared to the observations from Campos et al. (2021). This indicates that urban NO_x emissions in our model are highly underestimated in Southern Africa.

https://doi.org/10.5194/egusphere-2024-2576
Preprint. Discussion started: 19 September 2024

To test the sensitivity of simulated NO_2 concentration to urban emissions, we increased the NO_x emissions in the CEDSv2 inventory by a factor of 10, and the model results are shown in **Figure 9**. In Luanda, the Normalized Mean Bias (NMB) of simulated NO_2 concentrations will be decreased from -94% in the baseline simulation to -55%, while the changes of NO_2 in Humpata and Luena are very limited with an improvement of the NMB of only 5%. Even if when NO_x emission is scaled up by a factor of 20, the simulated NO_2 concentrations in Humpata and Luena are increased by only 11-21%. For Luanda, there is a NMB of -50% in modeled surface NO_2 with 10-fold NO_x emissions, and previous studies have shown that the GEOS-Chem model tends to underestimate observed surface NO_2 concentration by above 50% in urban air (Silvern et al., 2019), which may suggest that the upper limit of the underestimation in NO_x emissions from CEDSv2 inventory in Luanda is a factor of 10. But for Humpata and Luena, the CEDSv2 inventory is not capable to correctly estimate the anthropogenic sources, leading to the small sensitivity of simulated NO_2 concentration to perturbed urban emissions.

Although this study focused on ozone simulation, the comparison of model results against the valuable $PM_{2.5}$ measurements will be also meaningful to understand urban emissions in this region. **Figure 10** shows the time series of observed and simulated $PM_{2.5}$ concentrations in June-August 2023. The $PM_{2.5}$ concentrations observed at both the Humpata and Luanda sites were around 10 μg m^{-3}. The $PM_{2.5}$ concentrations at the Luena site were slightly higher compared to the other two sites, with median concentrations ranging from 10 μg m^{-3} to 70 μg m^{-3}. Lusaka is the capital of Zambia and the observed site is located within the urban area of Lusaka, where $PM_{2.5}$ concentrations were about 10 μg m^{-3} in June-July and then suddenly increased to about 20 μg m^{-3} in August. **Figure S5** shows the comparison of simulated and observed $PM_{2.5}$ concentrations, and the model can capture the day-to-day variation in $PM_{2.5}$ concentrations at Luena as well as Lusaka sites, with NMBs of -12% and 24% and correlation coefficients of 0.7 and 0.87, respectively. But in Luanda and Humpata, there is a large overestimation in simulated $PM_{2.5}$ concentration and a large proportion of $PM_{2.5}$ components is contributed by dust, possibly due to the influence of the Namib and Kalahari Deserts (Nyasulu et al., 2023). We excluded dust concentration in the calculation of total $PM_{2.5}$ concentration for the time being, due to its large uncertainties in the GEOS-Chem simulation (Weagle et al., 2018). After removing dust concentration, the NMB in the model will be reduced from 149% to 37% in Luanda.

In terms of $PM_{2.5}$ components, the highest contribution of OC to $PM_{2.5}$ concentrations is found at all the four sites, which can be attributed to the effects from biomass burning (Nyasulu et al., 2023). Secondary inorganic aerosols account for about 20% at Luanda and about 10% at other sites. In addition, we also compared the changes in $PM_{2.5}$ concentration at each site after scaling up anthropogenic NO_x emissions by a factor of 10, and found that $PM_{2.5}$ at the Luanda site can increase by up to 50 μg m^{-3}. In previous studies, changes in $PM_{2.5}$ concentrations in Southern Africa have often been attributed to BB (Nyasulu et al., 2023; Booyens et al., 2019). However, this study shows that anthropogenic

https://doi.org/10.5194/egusphere-2024-2576
Preprint. Discussion started: 19 September 2024

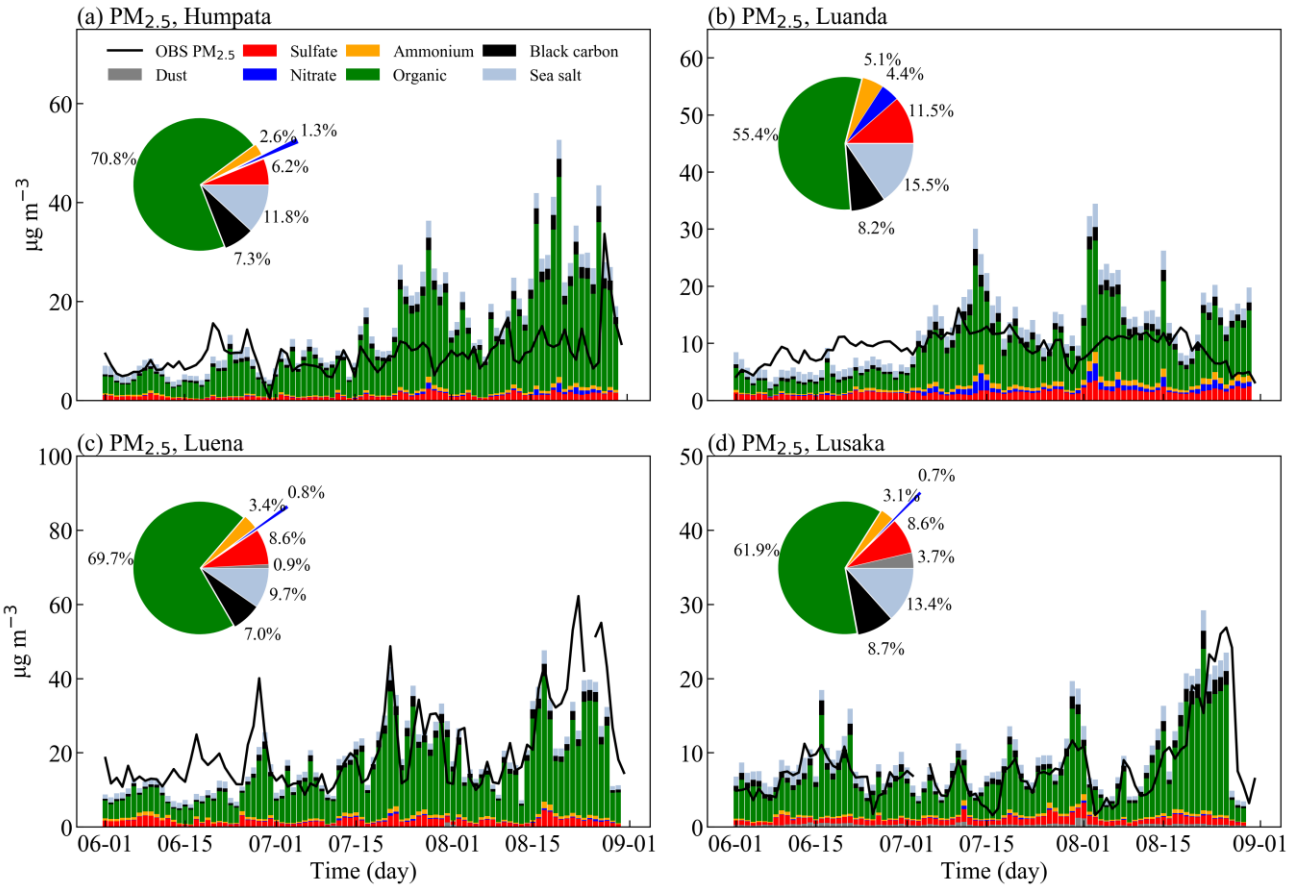

Figure 10. Comparison of simulated time series of $PM_{2.5}$ and its components against with the observed $PM_{2.5}$ (black line) during June-August 2023. (a) and (b) are for Humpata and Luanda, respectively, where we removed dust concentrations from the simulated $PM_{2.5}$ due to the large uncertainties in the model, and (c) and (d) are for Luena and Lusaka, respectively. The pie charts show the percentage contributions of each component to total $PM_{2.5}$ concentrations.

emissions in Luanda could also have a great impact on $PM_{2.5}$ concentrations, highlighting the underappreciated role of anthropogenic emissions in urban air quality over the Southern Africa.

We further explored the sensitivity of ozone concentration to perturbed NO_x emissions. **Figure S6** shows the response of ozone concentration at each site after anthropogenic NO_x was increased by 10 times. Relative to the baseline run, the ten-fold NO_x simulation can increase ozone concentrations by 0-10 ppb in the Humpata and Luean regions. However, in Luanda there was increased ozone in June but decreased ozone in July-August in response to ten-fold NO_x emissions, indicating

https://doi.org/10.5194/egusphere-2024-2576
Preprint. Discussion started: 19 September 2024

that ozone chemistry in Luanda may be likely shift into transition regime with increasing emissions. Again, these results confirm that the underestimation of anthropogenic emissions in the urban areas of Southern Africa now can have an important impact on local ozone assessment.

Although there is a lack of surface ozone observations in Southern Africa that can be directly compared with our model results, we can conclude from the model evaluation against surface NO_2 and $PM_{2.5}$ measurements: 1) the large underestimation in modeled urban scale NO_2 in Southern Africa is mainly due to high biases of NO_x emission in the CEDSv2 inventory, i.e., an underestimated by a factor of about 10 in Luanda and the misrepresentation of anthropogenic emissions estimates in Humpata and Luena, 2) the model is able to capture the observed variations in $PM_{2.5}$ concentrations in the areas that are less affected by dust, and 3) the bias in anthropogenic emission inventories can strongly affect the assessment of $PM_{2.5}$ and ozone concentrations in urban Southern Africa.

3.3.3 Model evaluation against satellite measurements

Satellite observations were further used to support the deduction of the underestimated urban emissions. As the capital of Angola, Luanda is of much higher anthropogenic emissions compared to other cities in Southern Africa. In the following, we focused on Luanda where satellite signals could be stronger to detect NO_x emissions. **Figure 11** shows the simulated and satellite-based NO_2 columns for fire season (July-August 2019) and non-fire season (January-February 2020), respectively. To minimize the effects from background levels, here the NO_2 values are the columns at Luanda minus the mean columns averaged over the sea downwind. For July-August 2019, the urban NO_2 enhancement in Luanda simulated by the model was 26% lower than that observed by the TROPOMI; for January-February 2020, the simulated NO_2 enhancement was underestimated by 61% compared to TROPOMI. The moderate underestimation during fire season (July-August 2019) in Luanda can be attributed to the long-term transport of BB emissions to the urban region. As suggested by TROPOMI satellite, therefore, NO_x emissions from CEDSv2 were underestimated by at least a factor of 2 in urban Luanda. At the same time, we find that the NO_2 enhancement in Luanda observed by OMI was 70% lower compared to TROPOMI and the OMI instrument cannot detect the high emissions in Luanda, demonstrating the advantage of TROPOMI instrument in observing regions like Southern Africa.

To further identify the key emission sectors in Luanda, we perturbed the NO_x emissions from three sectors (transportation, industrial, and energy) by a factor of 10 in **Figure 9a**. Surface NO_2 concentrations in Luanda responded better to changes in NO_x emissions from the energy and transportation sectors, with NMB reduced by 20% and 11%, respectively. **Figure S7** shows the NO_2 column changes in response to the emission perturbations. When all sources of NO_x emissions in the CEDSv2 inventory were increased by a factor of 10, the simulated NO_2 column enhancement in Luanda will be 3-4 times

https://doi.org/10.5194/egusphere-2024-2576
Preprint. Discussion started: 19 September 2024

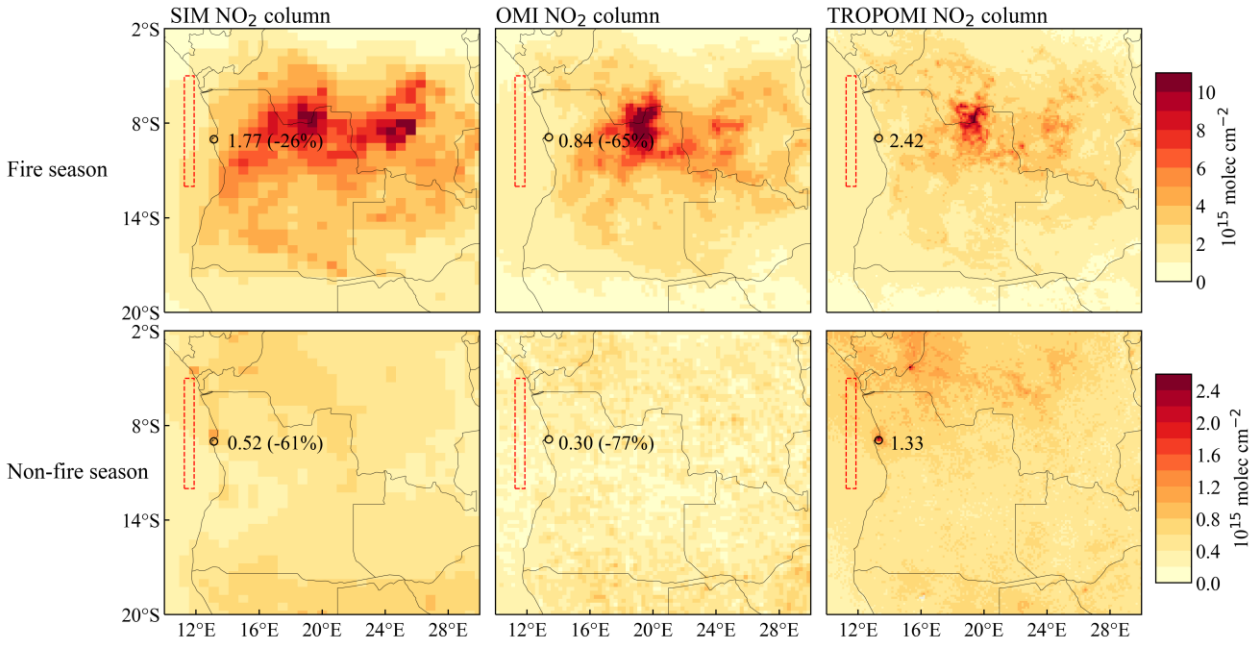

Figure 11. Spatial distribution of NO_2 columns from the model, OMI, and TROPOMI during the fire season (top) and non-fire season (bottom). Circles indicate the Luanda city and numbers around them indicate NO_2 column enhancement in the Luanda city. The dashed boxes indicate the downwind ocean region whose concentrations were subtracted to obtain the NO_2 column enhancement in Luanda. Percentages are their difference in Luanda relative to the observed NO_2 columns from TROPOMI.

the TROPOMI measurement. Namely, the ten-fold increase in NO_x emissions to be consistent with surface measurement cannot reconcile with satellite measurements. In addition, the response of NO_2 column in Luanda to sectoral perturbations in NO_x emissions is mainly linear (**Figure S7**). These model-satellite comparisons suggest an underestimation of NO_x emissions from CEDSv2 by at least a factor of 2 in urban Luanda.

Figure 12 shows the difference between anthropogenic NO_x emissions and satellite NO_2 columns for other cities with respect to Luanda. The selected cities are grid cells with high NO_x emissions in the CEDSv2 inventory. In Kinshasa (the capital of the DRC), anthropogenic NO_x emissions are 76% lower than those in Luanda, but their difference in satellite NO_2 columns was only 4-12%, suggesting that anthropogenic emissions from Kinshasa were also underestimated; In Lusaka (the capital of Zambia), its NO_2 columns were 55 % lower than those in Luanda while the difference is 76% in anthropogenic NO_x emissions. Combining satellite data with CEDSv2 NO_2 emissions provides additional evidence of the prevalent underestimation in anthropogenic NO_x emissions in major cities over Southern Africa.

https://doi.org/10.5194/egusphere-2024-2576
Preprint. Discussion started: 19 September 2024

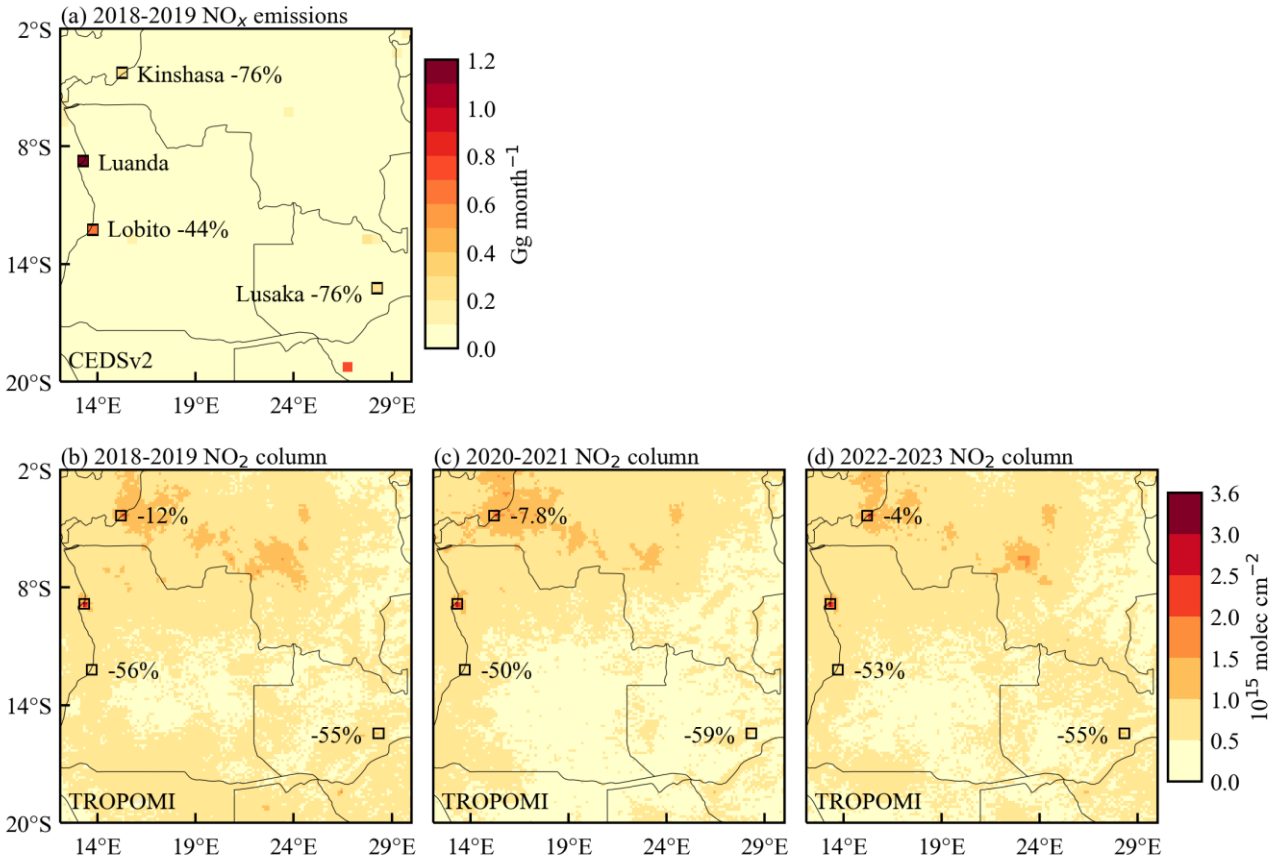

Figure 12. Anthropogenic NO_x emissions from CEDSv2 and NO_2 columns from TROPOMI in typical cities in Southern Africa. (a) Spatial distribution of NO_x emissions from the CEDSv2 inventory in March-April of 2018-2019. (b-d) Spatial distribution of NO_2 columns observed by TROPOMI in March-April, 2018-2023. All of the numbers in the plots are the percentage changes by taking Luanda as a reference.

4. Conclusions and discussion

In this study, we focused on Southern Africa where tropospheric ozone levels were thought extremely high but have been less studied. By integrating the nested GEOS-Chem model and the newly-available surface and satellite observations to evaluate the tropospheric ozone and its main drivers in Southern Africa. In particular, we quantified the impact of biomass burning (BB) on tropospheric ozone at the regional scale in Southern Africa and the effects of anthropogenic emissions in urban ozone level. This study provides a better understanding of the impacts of key emission sources on air quality modeling in Southern Africa, which will be also important for health risk assessment, climate change prediction, and

https://doi.org/10.5194/egusphere-2024-2576
Preprint. Discussion started: 19 September 2024

sustainable strategy development.

The anomalously high values of dry-season tropospheric ozone in Southern Africa are mainly caused by BB, but there is a large discrepancy of a factor of 2-3 in estimated BB emissions among different inventories. Comparison of model simulations against NO_2 satellite observations revealed that the widely-used GFED4.1 inventory tends to strongly overestimate NO_x emissions in Southern Africa, while model results with the QFED2 inventory were more consistent with observations. This is consistent with the finding by Anderson et al. (2021) that their model driven by the GFED4.1 inventory tended to overestimate NO_2 concentrations in the Africa , with a bias of about 100%. Consequently, the simulated regional surface MDA8 ozone was decreased from 74 ppb by GFED4.1 inventory to 56 ppb by QFED2 inventory, and accordingly the model bias in TCO was reduced from 14% to 2.3%. The modeled HCHO and CO columns are consistent between GFED4.1 and QFED2 inventories. Using the QFED2 inventory, we explored the impact of BB emission heights on ozone simulations and found that the effect of the vertical emission distribution was in the range of ± 2.4 ppb for surface MDA8 ozone and from -0.4 to 1.6 DU for TCO over Southern Africa; in contrast, the difference in BB aerosol emissions between the inventories could affect ozone simulation strongly through aerosol chemistry.

We conducted further sensitivity experiments using the QFED2 inventory to explore the contribution of anthropogenic emissions. Compared with surface NO_2 and $PM_{2.5}$ observations, we found that the CEDSv2 anthropogenic inventory likely underestimated anthropogenic emissions in typical Southern African cities by a factor of 2-10 and even incorrectly represented anthropogenic sources in some areas. Our study also found that the TROPOMI performs effectively in these low emission areas where there is a lack of observational data, and the OMI instrument is unable to capture urban-scale hotspots in NO_2 columns over Southern Africa. We also found that ozone and $PM_{2.5}$ concentrations are strongly influenced by the underestimated anthropogenic emissions. For example, a ten-fold increase in anthropogenic NO_x emissions can change ozone concentrations by up to 10 ppb and increase $PM_{2.5}$ concentrations by up to 50 μg m^{-3} in some cities.

Although several studies examined high ozone levels in Southern Africa (Meyer-Arnek et al., 2005; V. Clarmann et al., 2007), they only highlighted the role of biomass burning but overlooked the role of anthropogenic emissions. Although recent findings by Wiedinmyer et al. (2023) have pointed out the large uncertainties in bottom-up BB emissions, they failed to constrain the uncertainties due to the lack of observational data. Here we found that the difference among BB inventories can have a great impact on urban air quality assessment. In addition, with combined surface observations, satellite data and model simulations, we demonstrated for the first time that anthropogenic emission inventories are strongly low-biased in urban Southern Africa. It suggests the important impacts of anthropogenic emissions in Africa with increasing urbanization.

https://doi.org/10.5194/egusphere-2024-2576
Preprint. Discussion started: 19 September 2024

The rapid change in anthropogenic emissions is already affecting air pollution and health risks in Southern Africa (Health Effects Institute, 2022), as well as might have impacts on regional climate change (Fotso-Nguemo et al., 2023). Assessing and predicting the impacts of different emission sources on air quality and human health rely heavily on model simulations. The performance of these model estimations is significantly influenced by the accuracy of emission inventories. For example, our finding of overestimated biomass burning emissions and underestimated anthropogenic emissions can strongly affect the ozone source attribution over Southern Africa due to the nonlinear ozone chemistry. As shown in **Figure S8**, in the dry season of 2019, regional surface MDA8 ozone over Southern Africa was contributed by 11 ppb, 8.0 ppb, and 1.5 ppb from BB emissions, natural emissions (mainly biogenic VOC), and anthropogenic emissions, respectively. However, when anthropogenic NO_x emissions were increased by a factor of 10, estimated contributions from natural and anthropogenic emissions will be increased to 9.0 ppb and 3.3 ppb, respectively. In particular, the ozone source attribution spatially varies depending on the levels of anthropogenic NO_x emissions (**Figure 13**). This suggests the ignored but critical role of anthropogenic emissions in ozone levels over Southern Africa.

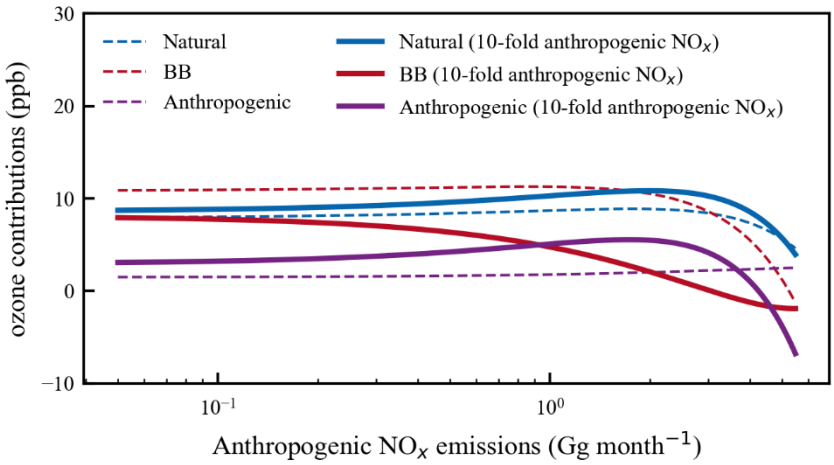

Figure 13. The simulated source contributions to surface ozone in July-August 2019 using the CEDSv2 emissions (dash lines) and 10-fold CEDSv2 NO_x emissions (solid lines). Here the natural emissions refer to the biogenic VOC and soil NO_x emissions. The x-axis is the anthropogenic NO_x emissions in each grid cell and the y-axis the corresponding ozone contributions estimated from the sensitivity simulations.

There are also some uncertainties and limitations in our assessment of the major drivers of high ozone over Southern Africa. Firstly, due to the lack of observational data on surface ozone and VOCs, the effect of anthropogenic emissions on surface ozone over Southern Africa was explored by only comparing surface NO_2 concentrations, which may lead to biases in determining ozone chemical formation. Secondly, although we have used ozonesonde data from Ascension Island

https://doi.org/10.5194/egusphere-2024-2576
Preprint. Discussion started: 19 September 2024

downwind of Southern Africa for comparison and the study by Jenkins et al. (2021) suggests that BB plumes in Southern Africa can have an impact on downwind regions, the long-range effects of BB emission on downwind urban regions were also not well validated due to the lack of vertical ozone measurement. Thirdly, although the GEOS-Chem model has been shown to be able to capture spatial and temporal variations of ozone and its precursors over typical urban regions (Travis and Jacob, 2019), it is still challenging to capture the urban scale air quality in Southern Africa. Without accurate bottom-up anthropogenic inventories, we highlight the importance of high-resolution satellite observations for understanding air quality in developing regions such as Southern Africa.

Overall, this work provides a comprehensive understanding of the drivers and uncertainties of tropospheric ozone in Southern Africa, particularly the overestimation in BB emissions and the underestimation of anthropogenic emission inventories. More importantly, with more frequent BB and rising anthropogenic emissions in Africa, this study highlights the urgency of establishing the surface network for air quality measurement over Southern Africa. The more accurate estimates of anthropogenic emission sources and more regular surface observations are the key to understand atmospheric chemistry over Southern Africa that is driven by rapidly changing anthropogenic and biomass burning emissions. The deepened understanding of major emission sources in Southern Africa will not only help us to provide a solid scientific basis for policymakers to effectively address air quality issues, but also will enhance the model capability to predict future air quality and climate change. In the future, anthropogenic air pollutants (e.g., NO_x emissions) in Southern Africa under future scenarios are projected to increase all the way by 2060 (**Figure S9**); along with more fires under a warming future, Southern Africa will be a hotspot suffering from complex atmospheric chemistry and climate issues, presenting a grand challenge to realize the Sustainable Development Goals for having a healthy, climate-friendly, and resilient development in Africa. Our study serves as a baseline understanding of these key emission sources which are key drivers for modelling future air quality, climate change, and their socioeconomic impacts.

Data availability. Daily real-time air quality indexes for NO_2 and $PM_{2.5}$ were obtained from the Worldwide Air Quality Index (https://aqicn.org/station). The Ascension Island's ozonesonde data from the Southern Hemisphere Additional Ozone Sounding network (https://tropo.gsfc.nasa.gov/shadoz/). The OMI satellite data for O_3, NO_2 and HCHO are available at https://disc.gsfc.nasa.gov/datasets/. The TROPOMI data for NO_2 are available at https://www.earthdata.nasa.gov/sensors/tropomi. The MODIS data for AOD are available at https://ladsweb.modaps.eosdis.nasa.gov/search/. The MOPITT data for CO are available at https://giovanni.gsfc.nasa.gov/giovanni/.

Competing interests. The authors declare that they have no conflict of interest.

Acknowledgements. We appreciate the efforts of the China Ministry of Ecology and Environment with respect to supporting the national surface observation network and the publishing of hourly air pollutant concentrations. We also thank the Atmospheric Chemistry Modeling group at Harvard University for developing and managing the GEOS-Chem model, and the high-performance computing cluster Xuanwu maintained by the Atmospheric Chemistry & Climate Group at NUIST.

Financial support. This research has been supported by the National Natural Science Foundation of China (grant no. 42293323), the National Key Research and Development Program of China (2022YFE0136100), the Natural Science Foundation of Jiangsu Province (BK20240035), and Jiangsu Carbon Peak and Neutrality Science and Technology Innovation fund (BK20220031).

References

Aghedo, A. M., Schultz, M. G., and Rast, S.: The influence of African air pollution on regional and global tropospheric ozone, Atmospheric Chemistry and Physics, 7, 1193-1212, https://doi.org/10.5194/acp-7-1193-2007, 2007.

Anderson, D. C., Duncan, B. N., Fiore, A. M., Baublitz, C. B., Follette-Cook, M. B., Nicely, J. M., and Wolfe, G. M.: Spatial and temporal variability in the hydroxyl (OH) radical: understanding the role of large-scale climate features and their influence on OH through its dynamical and photochemical drivers, Atmospheric Chemistry and Physics, 21, 6481-6508, https://doi.org/10.5194/acp-21-6481-2021, 2021.

Aucoin, C. and Bello-Schünemann, J.: African urban futures, Institute for Security Studies Papers, 2016, 1-36, https://hdl.handle.net/10520/EJC-b07eee7c0, 2016.

Balamurugan, V., Chen, J., Qu, Z., Bi, X., Gensheimer, J., Shekhar, A., Bhattacharjee, S., and Keutsch, F. N.: Tropospheric NO2 and O3 Response to COVID‐19 Lockdown Restrictions at the National and Urban Scales in Germany, Journal of Geophysical Research: Atmospheres, 126, https://doi.org/10.1029/2021JD035440, 2021.

Booyens, W., Beukes, J. P., Van Zyl, P. G., Ruiz-Jimenez, J., Kopperi, M., Riekkola, M.-L., Josipovic, M., Vakkari, V., and Laakso, L.: Summary of research paper published in Journal of Atmospheric Chemistry titled: Assessment of polar organic aerosols at a regional background site in southern Africa, Clean Air Journal, 29, https://doi.org/10.17159/2410-972X/2019/v29n1a10, 2019.

Boschetti, L. and Roy, D. P.: Defining a fire year for reporting and analysis of global interannual fire variability, Journal of Geophysical Research: Biogeosciences, 113, https://doi.org/10.1029/2008JG000686, 2008.

Bourgeois, I., Peischl, J., Neuman, J. A., Brown, S. S., Thompson, C. R., Aikin, K. C., Allen, H. M., Angot, H., Apel, E. C., Baublitz, C. B., Brewer, J. F., Campuzano-Jost, P., Commane, R., Crounse, J. D., Daube, B. C., DiGangi, J. P., Diskin,

https://doi.org/10.5194/egusphere-2024-2576
Preprint. Discussion started: 19 September 2024

G. S., Emmons, L. K., Fiore, A. M., Gkatzelis, G. I., Hills, A., Hornbrook, R. S., Huey, L. G., Jimenez, J. L., Kim, M., Lacey, F., McKain, K., Murray, L. T., Nault, B. A., Parrish, D. D., Ray, E., Sweeney, C., Tanner, D., Wofsy, S. C., and Ryerson, T. B.: Large contribution of biomass burning emissions to ozone throughout the global remote troposphere, Proceedings of the National Academy of Sciences, 118, https://doi.org/10.1073/pnas.2109628118, 2021.

Campos, P. M. D., Esteves, A. F., Leitão, A. A., and Pires, J. C. M.: Design of air quality monitoring network of Luanda, Angola: Urban air pollution assessment, Atmospheric Pollution Research, 12, 101128, https://doi.org/10.1016/j.apr.2021.101128, 2021.

Chang, I., Gao, L., Flynn, C. J., Shinozuka, Y., Doherty, S. J., Diamond, M. S., Longo, K. M., Ferrada, G. A., Carmichael, G. R., Castellanos, P., da Silva, A. M., Saide, P. E., Howes, C., Xue, Z., Mallet, M., Govindaraju, R., Wang, Q., Cheng, Y., Feng, Y., Burton, S. P., Ferrare, R. A., LeBlanc, S. E., Kacenelenbogen, M. S., Pistone, K., Segal-Rozenhaimer, M., Meyer, K. G., Ryoo, J.-M., Pfister, L., Adebiyi, A. A., Wood, R., Zuidema, P., Christopher, S. A., and Redemann, J.: On the differences in the vertical distribution of modeled aerosol optical depth over the southeastern Atlantic, Atmospheric Chemistry and Physics Discussions., 23, 4283-4309, https://doi.org/10.5194/acp-23-4283-2023, 2023.

Chen, Y., Hall, J., van Wees, D., Andela, N., Hantson, S., Giglio, L., van der Werf, G. R., Morton, D. C., and Randerson, J. T.: Multi-decadal trends and variability in burned area from the fifth version of the Global Fire Emissions Database (GFED5), Earth System Science Data, 15, 5227-5259, 10.5194/essd-15-5227-2023, 2023.

DeWitt, H. L., Gasore, J., Rupakheti, M., Potter, K. E., Prinn, R. G., Ndikubwimana, J. d. D., Nkusi, J., and Safari, B.: Seasonal and diurnal variability in O3, black carbon, and CO measured at the Rwanda Climate Observatory, Atmospheric Chemistry and Physics, 19, 2063-2078, https://doi.org/10.5194/acp-19-2063-2019, 2019.

Fajersztajn, L., Veras, M., Barrozo, L. V., and Saldiva, P.: Air monitoring coverage in low-income countries: an observational study, The Lancet, 384, https://doi.org/10.1016/s0140-6736(14)61877-8, 2014.

Fotso‐Nguemo, T. C., Weber, T., Diedhiou, A., Chouto, S., Vondou, D. A., Rechid, D., and Jacob, D.: Projected Impact of Increased Global Warming on Heat Stress and Exposed Population Over Africa, Earth's Future, 11, 10.1029/2022ef003268, 2023.

Fu, Y., Li, R., Hu, J., Wang, Y., and Duan, J.: Investigating the impacts of satellite fire observation accuracy on the top-down nitrogen oxides emission estimation in northeastern Asia, Environment International, 169, 107498, https://doi.org/10.1016/j.envint.2022.107498, 2022.

Gaudel, A., Cooper, O. R., Chang, K.-L., Bourgeois, I., Ziemke, J. R., Strode, S. A., Oman, L. D., Sellitto, P., Nédélec, P., Blot, R., Thouret, V., and Granier, C.: Aircraft observations since the 1990s reveal increases of tropospheric ozone at multiple locations across the Northern Hemisphere, Science Advances, 6, eaba8272, https://doi.org/10.1126/sciadv.aba8272, 2020.

Guenther, A. B., Jiang, X., Heald, C. L., Sakulyanontvittaya, T., Duhl, T., Emmons, L. K., and Wang, X.: The Model of

https://doi.org/10.5194/egusphere-2024-2576
Preprint. Discussion started: 19 September 2024

Emissions of Gases and Aerosols from Nature version 2.1 (MEGAN2.1): an extended and updated framework for modeling biogenic emissions, Geoscientific Model Development, 5, 1471-1492, https://doi.org/10.5194/gmd-5-1471-2012, 2012.

Health Effects Institute: The state of air quality and health impacts in Africa. A report from the state of global air initiative, 2022.

Hickman, J. E., Andela, N., Tsigaridis, K., Galy-Lacaux, C., Ossohou, M., Dammers, E., Van Damme, M., Clarisse, L., and Bauer, S. E.: Continental and Ecoregion - Specific Drivers of Atmospheric NO2 and NH3 Seasonality Over Africa Revealed by Satellite Observations, Global Biogeochemical Cycles, 35, e2020GB006916, https://doi.org/10.1029/2020gb006916, 2021.

Hoelzemann, J. J.: Global Wildland Fire Emission Modeling for Atmospheric Chemistry Studies, 2006.

Hoesly, R. M., Smith, S. J., Feng, L., Klimont, Z., Janssens-Maenhout, G., Pitkanen, T., Seibert, J. J., Vu, L., Andres, R. J., Bolt, R. M., Bond, T. C., Dawidowski, L., Kholod, N., Kurokawa, J.-i., Li, M., Liu, L., Lu, Z., Moura, M. C. P., O'Rourke, P. R., and Zhang, Q.: Historical (1750–2014) anthropogenic emissions of reactive gases and aerosols from the Community Emissions Data System (CEDS), Geoscientific Model Development, 11, 369-408, https://doi.org/10.5194/gmd-11-369-2018, 2018.

Jenkins, G. S., de Castro, V., Cunha, B., Fontanez, I., and Holzworth, R.: The Evolution of the Wave - One Ozone Maximum During the 2017 LASIC Field Campaign at Ascension Island, Journal of Geophysical Research: Atmospheres, 126, https://doi.org/10.1029/2020jd033972, 2021.

Jiang, Y., Zhou, L., and Raghavendra, A.: Observed changes in fire patterns and possible drivers over Central Africa, Environmental Research Letters, 15, https://doi.org/10.1088/1748-9326/ab9db2, 2020.

Julien, B., Véronique, Y., Corinne, G.-L., Marcellin, A., Aristide, A., Sékou, K., Cathy, L., Eric, G., Christelle, C., Money, O., Sylvain, G., and Julien, D.: A pilot study of gaseous pollutants' measurement (NO2, SO2, NH3, HNO3 and O3) in Abidjan, Côte d'Ivoire: contribution to an overview of gaseous pollution in African cities, Atmospheric Chemistry and Physics, 18, 5173-5198, https://doi.org/10.5194/acp-18-5173-2018, 2018.

Li, M., Yang, Y., Wang, H., Li, H., Wang, P., and Liao, H.: Summertime ozone pollution in China affected by stratospheric quasi-biennial oscillation, Atmospheric Chemistry and Physics, 23, 1533-1544, https://doi.org/10.5194/acp-23-1533-2023, 2023.

Liousse, C., Assamoi, E., Criqui, P., Granier, C., and Rosset, R.: Explosive growth in African combustion emissions from 2005 to 2030, Environmental Research Letters, 9, 035003, https://doi.org/10.1088/1748-9326/9/3/035003, 2014.

Liu, Y., Tang, Z., Abera, T., Zhang, X., Hakola, H., Pellikka, P., and Maeda, E.: Spatio-temporal distribution and source partitioning of formaldehyde over Ethiopia and Kenya, Atmospheric Environment, 237, https://doi.org/10.1016/j.atmosenv.2020.117706, 2020.

https://doi.org/10.5194/egusphere-2024-2576
Preprint. Discussion started: 19 September 2024

Lyu, X., Li, K., Guo, H., Morawska, L., Zhou, B., Zeren, Y., Jiang, F., Chen, C., Goldstein, A. H., Xu, X., Wang, T., Lu, X., Zhu, T., Querol, X., Chatani, S., Latif, M. T., Schuch, D., Sinha, V., Kumar, P., Mullins, B., Seguel, R., Shao, M., Xue, L., Wang, N., Chen, J., Gao, J., Chai, F., Simpson, I., Sinha, B., and Blake, D. R.: A synergistic ozone-climate control to address emerging ozone pollution challenges, One Earth, 6, 964-977, https://doi.org/10.1016/j.oneear.2023.07.004, 2023.

Marais, E. A. and Wiedinmyer, C.: Air Quality Impact of Diffuse and Inefficient Combustion Emissions in Africa (DICE-Africa), Environmental Science & Technology, 50, 10739-10745, https://doi.org/10.1021/acs.est.6b02602, 2016.

Mari, C. H., Cailley, G., Corre, L., Saunois, M., Attie, J. L., Thouret, V., and Stohl, A.: Tracing biomass burning plumes from the Southern Hemisphere during the AMMA 2006 wet season experiment, Atmospheric Chemistry and Physics, 8, 3951-3961, https://doi.org/10.5194/acp-8-3951-2008, 2008.

Marvin, M. R., Palmer, P. I., Latter, B. G., Siddans, R., Kerridge, B. J., Latif, M. T., and Khan, M. F.: Photochemical environment over Southeast Asia primed for hazardous ozone levels with influx of nitrogen oxides from seasonal biomass burning, Atmospheric Chemistry and Physics, 21, 1917-1935, https://doi.org/10.5194/acp-21-1917-2021, 2021.

Meyer-Arnek, J., Ladstätter-Weißenmayer, A., Richter, A., Wittrock, F., and Burrows, J. P.: A study of the trace gas columns of O3, NO2 and HCHO over Africa in September 1997, Faraday Discussions, 130, 387–405, https://doi.org/10.1039/b502106p, 2005.

Murray, C. J. L. and Aravkin, A. Y. and Zheng, P. and Abbafati, C. and Abbas, K. M. and Abbasi-Kangevari, M. and Abd-Allah, F. and Abdelalim, A. and Abdollahi, M. and Abdollahpour, I. and Abegaz, K. H. and Abolhassani, H. and Aboyans, V. and Abreu, L. G. and Abrigo, M. R. M. and Abualhasan, A. and Abu-Raddad, L. J. and Abushouk, A. I. and Adabi, M. and Adekanmbi, V. and Adeoye, A. M. and Adetokunboh, O. O. and Adham, D. and Advani, S. M. and Agarwal, G. and Aghamir, S. M. K. and Agrawal, A. and Ahmad, T. and Ahmadi, K. and Ahmadi, M. and Ahmadieh, H. and Ahmed, M. B. and Akalu, T. Y. and Akinyemi, R. O. and Akinyemiju, T. and Akombi, B. and Akunna, C. J. and Alahdab, F. and Al-Aly, Z. and Alam, K., et al.: Global burden of 87 risk factors in 204 countries and territories, 1990–2019: a systematic analysis for the Global Burden of Disease Study 2019, The Lancet, 396, 1223-1249, https://doi.org/10.1016/s0140-6736(20)30752-2, 2020.

Nikonovas, T., North, P. R. J., and Doerr, S. H.: Particulate emissions from large North American wildfires estimated using a new top-down method, Atmospheric Chemistry and Physics, 17, 6423-6438, https://doi.org/10.5194/acp-17-6423-2017, 2017.

Nyasulu, M., Thulu, F. G. D., and Alexander, F.: An assessment of four decades atmospheric PM2.5 trends in urban locations over Southern Africa using MERRA-2 reanalysis, Air Quality, Atmosphere & Health, 16, 2063-2084, https://doi.org/10.1007/s11869-023-01392-3, 2023.

Park, R. J., Jacob, D. J., Field, B. D., and Yantosca, R. M.: Natural and transboundary pollution influences on sulfate-

nitrate-ammonium aerosols in the United States: Implications for policy, Journal of Geophysical Research: Atmospheres, 109, 1-17, https://doi.org/10.1029/2003jd004473, 2004.

Pechony, O., Shindell, D. T., and Faluvegi, G.: Direct top-down estimates of biomass burning CO emissions using TES and MOPITT versus bottom-up GFED inventory, Journal of Geophysical Research: Atmospheres, 118, 8054-8066, https://doi.org/10.1002/jgrd.50624, 2013.

Petrenko, M., Kahn, R., Chin, M., Soja, A., Kucsera, T., and Harshvardhan: The use of satellite-measured aerosol optical depth to constrain biomass burning emissions source strength in the global model GOCART, Journal of Geophysical Research: Atmospheres, 117, 1-26, https://doi.org/10.1029/2012jd017870, 2012.

Qin, Y., Wang, H., Wang, Y., Lu, X., Tang, H., Zhang, J., Li, L., and Fan, S.: Wildfires in Southeast Asia pollute the atmosphere in the northern South China Sea, Science Bulletin, 69, 1011-1015, 10.1016/j.scib.2024.02.026, 2024.

Rémy, S., Veira, A., Paugam, R., Sofiev, M., Kaiser, J. W., Marenco, F., Burton, S. P., Benedetti, A., Engelen, R. J., Ferrare, R., and Hair, J. W.: Two global data sets of daily fire emission injection heights since 2003, Atmospheric Chemistry and Physics, 17, 2921-2942, https://doi.org/10.5194/acp-17-2921-2017, 2017.

Roy, R.: The cost of air pollution in Africa, https://doi.org/10.1787/18151949, 2016.

Shi, Y., Zang, S., Matsunaga, T., and Yamaguchi, Y.: A multi-year and high-resolution inventory of biomass burning emissions in tropical continents from 2001–2017 based on satellite observations, Journal of Cleaner Production, 270, https://doi.org/10.1016/j.jclepro.2020.122511, 2020.

Shi, Y., Matsunaga, T., Saito, M., Yamaguchi, Y., and Chen, X.: Comparison of global inventories of CO2 emissions from biomass burning during 2002–2011 derived from multiple satellite products, Environmental Pollution, 206, 479-487, https://doi.org/10.1016/j.envpol.2015.08.009, 2015.

Sicard, P., Agathokleous, E., Anenberg, S. C., De Marco, A., Paoletti, E., and Calatayud, V.: Trends in urban air pollution over the last two decades: A global perspective, Science of The Total Environment, 858, 160064, https://doi.org/10.1016/j.scitotenv.2022.160064, 2023.

Silvern, R. F., Jacob, D. J., Mickley, L. J., Sulprizio, M. P., Travis, K. R., Marais, E. A., Cohen, R. C., Laughner, J. L., Choi, S., Joiner, J., and Lamsal, L. N.: Using satellite observations of tropospheric NO2 columns to infer long-term trends in US NOx emissions: the importance of accounting for the free tropospheric NO2 background, Atmospheric Chemistry and Physics, 19, 8863-8878, https://doi.org/10.5194/acp-19-8863-2019, 2019.

Souri, A. H., Duncan, B. N., Strode, S. A., Anderson, D. C., Manyin, M. E., Liu, J., Oman, L. D., Zhang, Z., and Weir, B.: Enhancing Long-Term Trend Simulation of Global Tropospheric OH and Its Drivers from 2005-2019: A Synergistic Integration of Model Simulations and Satellite Observations, EGUsphere, 1-37, https://doi.org/10.5194/egusphere-2024-410, 2024.

Thompson, A. M., Doddridge, B. G., Witte , J. C., Hudson, R. D., Luke , W. T., Johnson, J. E., Johnson, B. J., Oltmans, S.

https://doi.org/10.5194/egusphere-2024-2576
Preprint. Discussion started: 19 September 2024

J., and Weller, R.: A Tropical Atlantic Paradox: Shipboard and Satellite Views of a Tropospheric Ozone Maximum and Wave-one in JanuaryFebruary 1999., Geophysical Research Letters, 27, 3317-3320, https://doi.org/10.1029/1999GL011273, 2000.

Tian, R., Ma, X., Jia, H., Yu, F., Sha, T., and Zan, Y.: Aerosol radiative effects on tropospheric photochemistry with GEOS-Chem simulations, Atmospheric Environment, 208, 82-94, https://doi.org/10.1016/j.atmosenv.2019.03.032, 2019.

Travis, K. R. and Jacob, D. J.: Systematic bias in evaluating chemical transport models with maximum daily 8 h average (MDA8) surface ozone for air quality applications: a case study with GEOS-Chem v9.02, Geoscientific Model Development, 12, 3641-3648, 10.5194/gmd-12-3641-2019, 2019.

v. Clarmann, T., Glatthor, N., Koukouli, M. E., Stiller, G. P., Funke, B., Grabowski, U., Hopfner, M., Kellmann, S., Linden, A., Milz, M., Steck, T., and Fischer, H.: MIPAS measurements of upper tropospheric C2H6 and O3 during the southern hemispheric biomass burning season in 2003, Atmospheric Chemistry and Physics, 7, 5861–5872, https://doi.org/10.5194/acp-7-5861-2007, 2007.

Van Der Werf, G. R., Randerson, J. T., Giglio, L., Van Leeuwen, T. T., Chen, Y., Rogers, B. M., Mu, M., Van Marle, M. J. E., Morton, D. C., Collatz, G. J., Yokelson, R. J., and Kasibhatla, P. S.: Global fire emissions estimates during 1997–2016, Earth System Science Data, 9, 697-720, https://doi.org/10.5194/essd-9-697-2017, 2017.

Vernooij, R., Giongo, M., Borges, M. A., Costa, M. M., Barradas, A. C. S., and Van Der Werf, G. R.: Intraseasonal variability of greenhouse gas emission factors from biomass burning in the Brazilian Cerrado, Biogeosciences, 18, 1375-1393, https://doi.org/10.5194/bg-18-1375-2021, 2021.

Vieira, I., Verbeeck, H., Meunier, F., Peaucelle, M., Sibret, T., Lefevre, L., Cheesman, A. W., Brown, F., Sitch, S., Mbifo, J., Boeckx, P., and Bauters, M.: Global reanalysis products cannot reproduce seasonal and diurnal cycles of tropospheric ozone in the Congo Basin, Atmospheric Environment, 304, 119773, https://doi.org/10.1016/j.atmosenv.2023.119773, 2023.

Vongruang, P., Wongwises, P., and Pimonsree, S.: Assessment of fire emission inventories for simulating particulate matter in Upper Southeast Asia using WRF-CMAQ, Atmospheric Pollution Research, 8, 921-929, https://doi.org/10.1016/j.apr.2017.03.004, 2017.

Wang, X., Fu, T. M., Zhang, L., Lu, X., Liu, X., Amnuaylojaroen, T., Latif, M. T., Ma, Y., Zhang, L., Feng, X., Zhu, L., Shen, H., and Yang, X.: Rapidly Changing Emissions Drove Substantial Surface and Tropospheric Ozone Increases Over Southeast Asia, Geophysical Research Letters, 49, e2022GL100223, https://doi.org/10.1029/2022gl100223, 2022.

Weagle, C. L., Snider, G., Li, C., van Donkelaar, A., Philip, S., Bissonnette, P., Burke, J., Jackson, J., Latimer, R., Stone, E., Abboud, I., Akoshile, C., Anh, N. X., Brook, J. R., Cohen, A., Dong, J., Gibson, M. D., Griffith, D., He, K. B., Holben, B. N., Kahn, R., Keller, C. A., Kim, J. S., Lagrosas, N., Lestari, P., Khian, Y. L., Liu, Y., Marais, E. A., Martins, J. V., Misra, A., Muliane, U., Pratiwi, R., Quel, E. J., Salam, A., Segev, L., Tripathi, S. N., Wang, C., Zhang, Q., Brauer,

M., Rudich, Y., et al.: Global Sources of Fine Particulate Matter: Interpretation of PM2.5 Chemical Composition Observed by SPARTAN using a Global Chemical Transport Model, Environmental Science & Technology, 52, 11670-11681, https://doi.org/10.1021/acs.est.8b01658, 2018.

Wells, K. C., Millet, D. B., Payne, V. H., Deventer, M. J., Bates, K. H., de Gouw, J. A., Graus, M., Warneke, C., Wisthaler, A., and Fuentes, J. D.: Satellite isoprene retrievals constrain emissions and atmospheric oxidation, Nature, 585, 225-233, https://doi.org/10.1038/s41586-020-2664-3, 2020.

Wiedinmyer, C., Akagi, S. K., Yokelson, R. J., Emmons, L. K., Al-Saadi, J. A., Orlando, J. J., and Soja, A. J.: The Fire INventory from NCAR (FINN): a high resolution global model to estimate the emissions from open burning, Geoscientific Model Development, 4, 625-641, https://doi.org/10.5194/gmd-4-625-2011, 2011.

Wiedinmyer, C., Kimura, Y., McDonald-Buller, E. C., Emmons, L. K., Buchholz, R. R., Tang, W., Seto, K., Joseph, M. B., Barsanti, K. C., Carlton, A. G., and Yokelson, R.: The Fire Inventory from NCAR version 2.5: an updated global fire emissions model for climate and chemistry applications, Geoscientific Model Development, 16, 3873-3891, https://doi.org/10.5194/gmd-16-3873-2023, 2023.

Williams, J. E., Scheele, M. P., van Velthoven, P. F. J., Cammas, J.-P., Thouret, V., Galy-Lacaux, C., and Volz-Thomas , A.: The influence of biogenic emissions from Africa on tropical tropospheric ozone during 2006: a global modeling study, Atmospheric Chemistry and Physics, 9, 5729–5749, https://doi.org/10.5194/acp-9-5729-2009, 2009.

Williams, J. E., Scheele, M. P., van Velthoven, P. F. J., Thouret, V., Saunois, M., Reeves, C. E., and Cammas, J. P.: The influence of biomass burning and transport on tropospheric composition over the tropical Atlantic Ocean and Equatorial Africa during the West African monsoon in 2006, Atmospheric Chemistry and Physics, 10, 9797-9817, https://doi.org/10.5194/acp-10-9797-2010, 2010.

Xu, R., Ye, T., Yue, X., Yang, Z., Yu, W., Zhang, Y., Bell, M. L., Morawska, L., Yu, P., Zhang, Y., Wu, Y., Liu, Y., Johnston, F., Lei, Y., Abramson, M. J., Guo, Y., and Li, S.: Global population exposure to landscape fire air pollution from 2000 to 2019, Nature, 621, 521-529, 10.1038/s41586-023-06398-6, 2023.

Xu, Z., Huang, X., Nie, W., Shen, Y., Zheng, L., Xie, Y., Wang, T., Ding, K., Liu, L., Zhou, D., Qi, X., and Ding, A.: Impact of Biomass Burning and Vertical Mixing of Residual‐Layer Aged Plumes on Ozone in the Yangtze River Delta, China: A Tethered‐Balloon Measurement and Modeling Study of a Multiday Ozone Episode, Journal of Geophysical Research: Atmospheres, 123, 11786-11803, https://doi.org/10.1029/2018jd028994, 2018.

Yang, J., Kang, S., Hu, Y., Chen, X., and Rai, M.: Influence of South Asian Biomass Burning on Ozone and Aerosol Concentrations Over the Tibetan Plateau, Advances in Atmospheric Sciences, 39, 1184-1197, https://doi.org/10.1007/s00376-022-1197-0, 2022.

Yue, X., Hu, Y., Tian, C., Xu, R., Yu, W., and Guo, Y.: Increasing impacts of fire air pollution on public and ecosystem health, The Innovation, 5, 10.1016/j.xinn.2024.100609, 2024.

https://doi.org/10.5194/egusphere-2024-2576
Preprint. Discussion started: 19 September 2024

Zhang, T., Wooster, M., de Jong, M., and Xu, W.: How Well Does the 'Small Fire Boost' Methodology Used within the GFED4.1s Fire Emissions Database Represent the Timing, Location and Magnitude of Agricultural Burning?, Remote Sensing, 10, 823, https://doi.org/10.3390/rs10060823, 2018.

Zhang, Y., West, J. J., Emmons, L. K., Flemming, J., Jonson, J. E., Lund, M. T., Sekiya, T., Sudo, K., Gaudel, A., Chang, K. L., Nédélec, P., and Thouret, V.: Contributions of World Regions to the Global Tropospheric Ozone Burden Change From 1980 to 2010, Geophysical Research Letters, 48, 10.1029/2020gl089184, 2021.